

Partial identification and unmeasured confounding with multiple treatments and multiple outcomes

Suyeon Kang* Alexander Franks† Michelle Audirac‡ Danielle Braun§ Joseph Antonelli¶

Abstract

Estimating the health effects of multiple air pollutants is a crucial problem in public health, but one that is difficult due to unmeasured confounding bias. Motivated by this issue, we develop a framework for partial identification of causal effects in the presence of unmeasured confounding in settings with multiple treatments and multiple outcomes. Under a factor confounding assumption, we show that joint partial identification regions for multiple estimands can be more informative than considering partial identification for individual estimands one at a time. We show how assumptions related to the strength of confounding or magnitude of plausible effect sizes for one estimand can reduce the partial identification regions for other estimands. As a special case of this result, we explore how negative control assumptions reduce partial identification regions and discuss conditions under which point identification can be obtained. We develop novel computational approaches to finding partial identification regions under a variety of these assumptions. We then estimate the causal effect of $PM_{2.5}$ components on a variety of public health outcomes in the United States Medicare cohort, where we find that, in particular, the detrimental effect of black carbon is robust to the potential presence of unmeasured confounding bias.

Keywords: Causal inference, Partial identification, Sensitivity analysis, Multiple treatments, Multiple Outcomes, Air pollution, Environmental mixtures.

1 Introduction

Understanding the health effects of air pollution is a critically important problem in public health research. There is a vast literature that indicates substantial detrimental impacts of air pollution (Cohen et al., 2017; Burnett et al., 2018; Manisalidis et al., 2020). This has helped inform regulatory policy on how to reduce air pollution, and it is important to obtain accurate estimates of the impact of these policies as both the costs and benefits of these policies are in the billions of dollars (Portney, 1990). Due to the importance of this problem and the need for policy-relevant estimates of the impacts of air pollution, there has been a push towards causal inference approaches in environmental epidemiology (Dominici and Zigler, 2017; Carone et al., 2020; Sommer et al., 2021).

*Assistant Professor, Department of Statistics and Data Science, University of Central Florida (Email: suyeon.kang@ucf.edu)

†Associate professor, Department of Statistics and Applied Probability, University of California, Santa Barbara (Email: afranks@pstat.ucsb.edu)

‡Senior Data Science Specialist, Department of Biostatistics, Harvard T.H. Chan School of Public Health (Email: maudirac@hsph.harvard.edu)

§Principal research scientist, Department of Biostatistics, Harvard T.H. Chan School of Public Health, Department of Data Science, Dana-Farber Cancer Institute (Email: dbraun@mail.harvard.edu)

¶Assistant Professor, Department of Statistics, University of Florida (Email: jantonelli@ufl.edu)

Causal inference in these settings is difficult for a multitude of reasons, but arguably the biggest impediment to assessing the causal effect of environmental exposures is the potential for unmeasured confounding bias. In the presence of unmeasured confounding, causal effects are not identifiable, and consistent estimation of them is not possible without additional information or assumptions. In some settings, a natural experiment is available that helps to alleviate issues stemming from unmeasured confounding (Rich, 2017). Examples include pollution reductions due to the Olympic games in Atlanta or Beijing (Huang et al., 2015) or the decommissioning of power plants leading to large reductions in pollution for nearby areas (Luechinger, 2014). Other work has looked to leverage recent advancements in double negative control designs to estimate causal effects in a manner that is robust to unmeasured confounding (Schwartz et al., 2023). Generally, however, natural experiments or other designs that alleviate concerns about unmeasured confounding are not always available. Given the importance of this problem in air pollution research and its ubiquity in the broader causal inference framework, we develop methods for partial identification of causal effects under unmeasured confounding. We pay particular attention to settings with multiple treatments and outcomes, which we show offer significant advantages for partial identification.

Historically, the most common approach for assessing the unmeasured confounding assumption is sensitivity analysis, which dates back at least as far as Cornfield et al. (1959) who argued that there is a causal relationship between smoking and lung cancer. A central goal of sensitivity analysis is to provide bounds on causal estimands that account for potential biases stemming from unmeasured confounding. In simple cases such as with bounded outcomes, general bounds for causal effects can be estimated (Manski, 1990), though typically bounds are estimated based on sensitivity parameters governing the strength of association between the unmeasured confounders and either the treatment or outcome. One approach is to posit a sensitivity parameter for the relationship between the unmeasured variable and treatment, while assuming the worst-case scenario that the unmeasured confounder and outcome are nearly co-linear (Rosenbaum, 1987, 1988, 1991, 2002b,a). Other approaches have two sensitivity parameters that govern the strength of association between the unmeasured variable and both the treatment and outcome. These parameters are intended to be interpretable so that one can reason potential values for them. This can be done by letting them be parameters of a regression model (Rosenbaum and Rubin, 1983; McCandless et al., 2007), parameters dictating relative risks (VanderWeele and Ding, 2017; Ding and VanderWeele, 2016), or partial R^2 values between the unmeasured variable and the treatment or outcome (Imbens, 2003; Small, 2007; Veitch and Zaveri, 2020; Cinelli and Hazlett, 2020; Freidling and Zhao, 2022; Chernozhukov et al., 2022).

While much of the existing work focuses on a single treatment variable, recent work has examined settings with multiple treatments (Wang et al., 2017; Miao et al., 2022; Kong et al., 2022; Zheng et al., 2021, 2022). Under certain assumptions about the nature of confounding, partial R^2 values between the unmeasured confounders and treatment can be identified from the observed data. In some cases, such as sparsity in the effects of the treatment on the outcome, the causal effects are even identifiable in this setting (Wang et al., 2017; Miao et al., 2022). Another example is Kong et al. (2022), which shows identifiability with multiple treatments and a binary outcome under the assumption the treatments are independent given a common unmeasured confounder. Similar results have been shown in the multi-outcome setting (Zhou et al., 2020; Zheng et al., 2023). Recent work in Wu et al. (2023) has extended these ideas in a number of directions, in particular to the multiple treatment and multiple outcome setting, where causal identification can be obtained under certain conditional independence assumptions related to those seen in the proximal causal inference literature (Kuroki and Pearl, 2014; Tchetgen Tchetgen et al., 2024). In general, the presence of multiple treatments or outcomes can provide substantial benefits, which is particularly important

for air pollution research as there are large numbers of environmental exposures of interest, and they are potentially associated with a variety of adverse health outcomes. As mentioned above, one can obtain identification in these settings even with unmeasured confounding, albeit under fairly strong, restrictive assumptions. Under weaker assumptions, one can potentially obtain partial identification of treatment effects, where only a set of values of the causal effect is identified, which is the focus of this work.

In this paper, we develop a general partial identification framework for scenarios with multiple treatments and multiple outcomes to study whether the estimated health effects of air pollution are robust to the presence of unmeasured confounding bias. While motivated by settings in air pollution epidemiology, this work has broader implications for partial identification of causal effects with multiple treatments and outcomes. Under a factor confounding assumption, we are able to identify worst-case bounds for causal effects without any additional sensitivity parameters. Further, we show that additional assumptions about the bias, effect size or strength of confounding on any set of estimands can decrease the worst-case bounds for other causal estimands, highlighting the benefit of joint inference over one-at-a-time sensitivity analysis. Specifically, we illustrate two different classes of assumptions which we can be used to reduce the joint partial identification region for all causal estimands: 1) assumptions about the magnitude of effect sizes (or bias), or 2) assumptions about the strength of confounding, e.g., by bounding the fraction of outcome variance and treatment variance explained by unmeasured confounders (given measured confounders). We provide theoretical results for these strategies and develop novel computational tools for characterizing partial identification regions. We then estimate the health effects of multivariate air pollution exposures in a nationwide study in the United States using Medicare claims data. We utilize the aforementioned approaches to study whether the adverse health effects of air pollution are robust to unmeasured confounding, and quantify how much the partial identification regions for causal effects of interest change under different assumptions about the strength of confounding.

2 Motivating study of the health effects of air pollution

Understanding the health effects of air pollution is a critically important problem in public health research. While there is a large literature showing adverse health effects of air pollution, nearly all of the research is observational, and therefore relies on certain untestable assumptions. A large number of these studies assume that the observed covariates contain all confounders of the exposure-outcome relationship. Due to the importance of this public health problem, and the impact these studies have on environmental regulatory policy, it is important to assess whether these findings are robust to unmeasured confounding bias. This manuscript works to develop methodology to estimate the causal effect of ozone and specific components of PM_{2.5} on a variety of health outcomes, while accounting for the possibility that these are subject to unmeasured confounding bias.

To study this question, we use claims data from Medicare Fee-for-Service enrollees over the age of 65 that were enrolled in the years 2000 to 2016 obtained from the Centers of Medicare and Medicaid Services. For each enrollee we have information on their age, sex, race, and whether they are Medicaid eligible, which functions as a proxy for low socioeconomic status, as well as their residential zip code. In addition to these individual level characteristics, we have a number of area level characteristics that are available through the United States Census Bureau and the Center for Disease Control's Behavioral Risk Factor Surveillance System. These include covariates such as average body mass index, education level, population density, smoking rates, median household income and house value, and the percentage of owner occupied housing. We also adjust for mete-

orological variables, such as temperature and precipitation rates from the National Climatic Data Center.

In our analysis, we focus on six different air pollution exposures from two distinct publicly available sources: we obtain estimates of ammonium (NH_4), nitrates (NO_3), and sulfate (SO_4) levels on a $(0.01^\circ \times 0.01^\circ)$ grid from the Atmospheric Composition Analysis Group (Van Donkelaar et al., 2019) and we obtain estimates of elemental carbon (EC), organic carbon (OC), and ozone (O_3) on a 1km by 1km daily grid from the Socioeconomic Data and Applications Center (Di et al., 2021; Requia et al., 2021). These exposures are aggregated to the zip code level so that they can be linked to the residential zip code obtained from Medicare, and are additionally aggregated to the yearly level as we are examining long term exposure to pollution. The outcomes of interest consist of zip code level hospitalization rates for anemia, COPD, lung cancer, stroke, and asthma, which are obtained based on ICD9/10 diagnosis codes. Additionally, we have access to negative control outcomes, which are hospitalization rates in the year prior to exposure. We focus on using hospitalization rates for COPD in the prior year as a negative control outcome. Our unit of analysis is a United States zip code, and our data consists of all zip codes in the contiguous United States. All covariates are aggregated up to the zip code level by taking their averages or proportions within each zip code. Similar data sources have been used previously to provide impactful, large-scale estimates of the health effects of $\text{PM}_{2.5}$ (Di et al., 2017). Critically, these results have relied on the no unmeasured confounding assumption, and in this work we aim to clarify the extent to which these effects are robust to unmeasured confounding. This will provide environmental regulators with improved scientific evidence on the nature of the relationship between air pollution and public health.

3 Notation and estimands

Throughout, we observe (Y_i, T_i, X_i) for $i = 1, \dots, n$. Here, $T = (T_1, \dots, T_k)^\top$ denotes a vector of k treatments, $Y = (Y_1, \dots, Y_q)^\top$ denotes a vector of q outcomes, and $X = (X_1, \dots, X_l)^\top$ denotes a vector of l pre-treatment covariates, respectively. Throughout, we use the terms exposures and treatments interchangeably when referring to T . Under the potential outcome framework (Rubin, 1974; Splawa-Neyman et al., 1990), we let $Y(t)$ denote the potential outcome that would have been observed had the treatment T been set to t . Our goal throughout will be to utilize the observed data to estimate the population average treatment effect (PATE), for a linear combination of outcomes $a^\top Y$, defined as

$$\text{PATE}_{a, t_1, t_2} := E[a^\top Y(t_1) - a^\top Y(t_2)]$$

for some t_1, t_2 . If unmeasured confounders U were observed along with X , we could nonparametrically identify the causal effect from the observed data under the following assumption:

Assumption 1.

1. *SUTVA (Stable Unit Treatment Value Assumption): There is no interference between units and there is only a single version of each assigned treatment.*
2. *Latent ignorability: $Y(t) \perp\!\!\!\perp T \mid (U, X)$ for all t .*
3. *Latent positivity: $f(t \mid U = u, X = x) > 0$ for all possible values of t , x , and u . Here, $f(\cdot)$ represents the conditional density function of T given (X, U) .*

The SUTVA assumption ensures that $Y(t)$ is well-defined and that $Y = Y(t)$ if $T = t$, which links the observed data to potential outcomes. The latent ignorability assumption states that X and

U contain all common causes of T and Y . The latent positivity assumption, also referred to as overlap, assures that there is a positive probability that each unit receives any treatment value t given both X and U . Under these assumptions, we can identify the causal effect of interest using $E[Y(t)] = E_{X,U}[E(Y|T = t, X, U)]$.

Note that our identification assumptions include unmeasured confounders U , which are not observed, and therefore the causal effect is not identifiable without further assumptions, as the effect of T on Y may be confounded by U even after conditioning on X . Our goal in this manuscript is to derive partial identification regions for the causal effect that account for the potential presence of unmeasured confounders when we have both multiple treatments and multiple outcomes under varying assumptions about the unmeasured variables. For now, we assume the number of unmeasured confounders m is known and fixed. We discuss estimation of m in Appendix C.

4 Partial Identification and Factor Confounding

In this section, we first show that the causal effect of interest is not point-identified in our setting, but the range of possible values for the causal effect can be characterized by quantities that, under a factor confounding assumption, can be identified in the multi-treatment and multi-outcome setting.

4.1 Factor models with multivariate treatments and outcomes

For ease of exposition, we do not include observed covariates X in this section, though all results hold analogously when conditioning on X . Throughout, we consider the latent variable models that are described by the following assumptions.

Assumption 2 (Confounder homoskedasticity). *Let $E[U|T = t] := \mu_{u|t}$ and $Var(U|T = t) := \Sigma_{u|t}$ be the m -dimensional mean and $m \times m$ covariance matrix of latent confounders given treatments. Assume that the confounders are homoskedastic in t , meaning that $\Sigma_{u|t}$ is invariant to the level of t .*

Assumption 3 (Outcomes are linear in latent confounders). *The mean of the outcome is linear in the unmeasured confounders with mean*

$$E[Y|T, U] = g(T) + \Gamma \Sigma_{u|t}^{-1/2} U. \quad (1)$$

with $\Gamma \in \mathbb{R}^{q \times m}$ and q -dimensional diagonal variance $Var(Y|T, U) := D$.

Note that if we had observed covariates X , they would be placed inside of the $g(\cdot)$ function along with T thereby allowing for arbitrary relationships between the observed variables. We only require a specific structure for the effect of the unobserved confounders on the outcome. Assumptions 2 and 3 imply that the observed outcome moments are

$$E(Y|T = t) = \check{g}(t) = g(t) + \Gamma \Sigma_{u|t}^{-1/2} \mu_{u|t}, \quad (2)$$

$$Var(Y|T = t) = \Gamma \Gamma^\top + D. \quad (3)$$

Given that our estimand of interest is

$$PATE_{a,t_1,t_2} := E[a^\top Y(t_1) - a^\top Y(t_2)] \quad (4)$$

$$= a^\top g(t_1) - a^\top g(t_2), \quad (5)$$

Equation (2) shows that the bias from ignoring unmeasured confounders, U is

$$\begin{aligned}\text{Bias}_{a,t_1,t_2} &= [a^\top \check{g}(t_1) - a^\top \check{g}(t_2)] - \text{PATE}_{a,t_1,t_2} \\ &= a^\top \Gamma \Sigma_{u|t}^{-1/2} (\mu_{u|t_1} - \mu_{u|t_2}).\end{aligned}\quad (6)$$

While the bias term in equation (6) is not identifiable in the absence of data on U , we can derive upper bounds for this bias that are themselves identifiable under certain assumptions about the unmeasured confounders.

Theorem 1. *Given Assumptions 1–3, the confounding bias of PATE_{a,t_1,t_2} can be bounded as*

$$\text{Bias}_{a,t_1,t_2}^2 \leq \|a^\top \Gamma\|_2^2 \|\Sigma_{u|t}^{-1/2} (\mu_{u|t_1} - \mu_{u|t_2})\|_2^2,$$

where the right-hand side is the worst-case bias of the naive estimator and is achieved when $a^\top \Gamma$ is colinear with $\Sigma_{u|t}^{-1/2} \mu_{u|\Delta t}$.

The proof of the theorem is given in Appendix A. $a^\top \Gamma$ can be viewed as the strength of association between the unmeasured variables U and the outcome, while $\Sigma_{u|t}^{-1/2} \mu_{u|\Delta t}$ is the scaled difference in unmeasured confounder means when treatment is shifted from t_1 to t_2 and represents the strength of association between the unmeasured confounders and treatment. This result implies that the true treatment effect lies in the interval

$$a^\top [\check{g}(t_1) - \check{g}(t_2)] \pm \|a^\top \Gamma\|_2 \|\Sigma_{u|t}^{-1/2} \mu_{u|\Delta t}\|_2. \quad (7)$$

While the confounding bias itself is not identifiable, it can be shown that this bound is identified for some latent variable models.

In particular, in this work we focus on the probabilistic principal component analysis model to describe variation among treatments:

$$U = \epsilon_U \quad (8)$$

$$T = BU + \epsilon_T \quad (9)$$

where $B \in \mathbb{R}^{k \times m}$, $\epsilon_U \sim N_m(0, I_m)$ and $\epsilon_T \sim N_k(0, \Sigma_{t|u})$ with $\Sigma_{t|u}$ being a diagonal matrix. This model implies the conditional confounder distribution is

$$f(u|T = t) \sim N_m(\mu_{u|t}, \Sigma_{u|t}) \quad (10)$$

where

$$\begin{aligned}\mu_{u|t} &= B^\top (BB^\top + \Sigma_{t|u})^{-1} t, \\ \Sigma_{u|t} &= I_m - B^\top (BB^\top + \Sigma_{t|u})^{-1} B.\end{aligned}$$

This leads to our main assumption, which will allow us to identify bounds on the causal effect.

Assumption 4 (Factor confounding assumption). *The treatments are generated by (8)–(9) and U represents potential confounders in the sense that they are possible causes of T and Y and are not themselves caused by T or Y . Additionally, we assume the following conditions are satisfied.*

1. *If any row of Γ is deleted, there remain two disjoint submatrices of rank m , where $m = \text{rank}(\Gamma)$*
2. *If any row of B is deleted, there remain two disjoint submatrices of rank m , where $m = \text{rank}(B)$.*

This assumption implies that the factor loadings Γ and B are identifiable up to rotation. In order for Γ to be identified up to rotation, it must be true that each confounder is correlated with at least three outcomes, and that $(q - m)^2 - q - m \geq 0$, where q is the number of outcomes in the data and m is the number of unobserved confounders. Likewise, the assumption implies that for B to be identified up to rotation, we require that each confounder is correlated with at least three treatments, and that $(k - m)^2 - k - m \geq 0$, where k is the number of treatments. Factor confounding leads to the following result.

Theorem 2. *Given Assumptions 1–4, both $\|a^\top \Gamma\|_2^2$ and $\|\Sigma_{u|t}^{-1/2} \mu_{u|\Delta t}\|_2^2$ are identifiable and thus the bound on $Bias_{a,t_1,t_2}$, given by $\|a^\top \Gamma\|_2^2 \|\Sigma_{u|t}^{-1/2} \mu_{u|\Delta t}\|_2^2$, is also identifiable. Further, for any orthogonal matrix $\tilde{\Gamma}$ satisfying $\tilde{\Gamma}\tilde{\Gamma}^\top = \Gamma\Gamma^\top$ and \tilde{B} , satisfying $\tilde{B}\tilde{B}^\top = BB^\top$ there exists an $m \times m$ orthonormal matrix, R , such that*

$$Bias_{a,t_1,t_2} = a^\top \tilde{\Gamma} R \tilde{\Sigma}_{u|t}^{-1/2} \tilde{\mu}_{u|\Delta t},$$

where $\tilde{\mu}_{u|\Delta t}$ and $\tilde{\Sigma}_{u|t}^{-1/2}$ are the matrices implied by the particular value of \tilde{B} . The equivalence class of matrices $\tilde{\Gamma}$ and \tilde{B} are identifiable, so the only unidentified component of the bias is R .

One consequence of this result is that without loss of generality, we can let $\tilde{B} = B$ so that we can simply write $\tilde{\Sigma}_{u|t}^{-1/2} = \Sigma_{u|t}^{-1/2}$, and $\tilde{\mu}_{u|\Delta t} = \mu_{u|\Delta t}$. For the purposes of exposition, we then let $\Gamma = \tilde{\Gamma}R$.

Note that Assumption 4 states that U are in fact confounders. The factor models reflect residual correlation in the treatments and outcomes, which we assume is driven entirely by unmeasured confounders. While this correlation could also be due to nonconfounding sources (e.g., predictors of only treatment or only outcome, or mediators), the bias bound in Theorem 1 still provides valid conservative bounds on the causal effects, as we will over-estimate the extent to which unmeasured confounding is biasing our estimates.

5 Joint Partial identification regions under additional constraints

Theorem 2 highlights that with a factor confounding assumption, we can bound the causal effects for all estimands in (7) in settings with multiple treatments and multiple outcomes. However, in some contexts, these bounds are too wide to be practically useful without additional assumptions. This occurs in our motivating example in Section 7 as the bounds contain all plausible (and some implausible) effects of air pollution. However, there are additional benefits that come from considering the joint partial identification region for multiple estimands. Importantly, the joint partial identification region is *not* simply the Cartesian product of the marginal bounds, as the worst-case bounds for multiple estimands cannot be simultaneously attained. In many instances, assumptions about the bias on one estimand can be highly informative about the bias of other estimands (see Figure 1).

By way of example, suppose that we are interested in two estimands, $PATE_{a_1,t_1,t_2}$ and $PATE_{a_2,t_1,t_2}$, which correspond to distinct outcomes, a_1 and a_2 , but the same treatment contrast (t_2 vs t_1). The degree to which assumptions about $PATE_{a_1,t_1,t_2}$ inform the partial identification region for $PATE_{a_2,t_1,t_2}$ is driven in part by the inner product of $a_1^\top \Gamma$ and $a_2^\top \Gamma$. This is illustrated in Figure 1 where we can see a strong dependence in the bivariate partial identification region when $|\langle a_1^\top \Gamma, a_2^\top \Gamma \rangle|$ is large (Figure 1, right). Even when $a_1^\top \Gamma$ and $a_2^\top \Gamma$ are orthogonal, the magnitude of the bias for one estimand is weakly informative about the magnitude of the bias for the other (Figure 1, left).

We formalize these ideas in the following proposition, which characterizes the partial identification region for one estimand as a function of the bias of another.

Proposition 1. *Given Assumptions 1–4, if we further assume that $\text{Bias}_{a_1, t_1, t_2} = \beta_1$, then the partial identification region for a different outcome with the same treatment contrast, $\text{Bias}_{a_2, t_1, t_2}$, is given by*

$$\begin{aligned} \text{Bias}_{a_2, t_1, t_2} &\in \\ \beta_1 \left(\frac{a_1^\top \Gamma \Gamma^\top a_2}{a_1^\top \Gamma \Gamma^\top a_1} \right) &\pm \sqrt{a_2^\top \Gamma \Gamma^\top a_2 - \frac{(a_1^\top \Gamma \Gamma^\top a_2)^2}{a_1^\top \Gamma \Gamma^\top a_1}} \left\| \left(I - \frac{\Gamma^\top a_1 a_1^\top \Gamma}{a_1^\top \Gamma \Gamma^\top a_1} \right) \Sigma_{u|t}^{-1/2} \mu_{u|\Delta t} \right\|_2 \end{aligned} \quad (11)$$

$$\subseteq \left[-\|a_2^\top \Gamma\|_2 \|\Sigma_{u|t}^{-1/2} \mu_{u|\Delta t}\|_2, \quad \|a_2^\top \Gamma\|_2 \|\Sigma_{u|t}^{-1/2} \mu_{u|\Delta t}\|_2 \right] \quad (12)$$

This conditional partial identification region (11) is contained in the marginal identification region (12), can be much shorter in length, and may have a different center. For one, given $\text{Bias}_{a_1, t_1, t_2} = \beta_1$, the identification region for $\text{Bias}_{a_2, t_1, t_2}$ is no longer necessarily centered at zero. The magnitude of the bias correction depends on β_1 as well as $\langle a_1^\top \Gamma, a_2^\top \Gamma \rangle$. The width of the partial identification region in (11) is the product of two terms. The first term is smallest when $|\langle a_1^\top \Gamma, a_2^\top \Gamma \rangle|$ is large and reaches zero when $a_1^\top \Gamma$ and $a_2^\top \Gamma$ are collinear. In the air pollution setting, it is plausible that $|\langle a_1^\top \Gamma, a_2^\top \Gamma \rangle|$ is large, as common unmeasured confounders are likely to affect multiple public health outcomes. The second term is small when $\text{Bias}_{a_1, t_1, t_2}$ is large in magnitude. This is because $\left(I - \frac{\Gamma^\top a_1 a_1^\top \Gamma}{a_1^\top \Gamma \Gamma^\top a_1} \right) \Sigma_{u|t}^{-1/2} \mu_{u|\Delta t}$ is the projection of $\Sigma_{u|t}^{-1/2} \mu_{u|\Delta t}$ onto the space orthogonal to $a_1^\top \Gamma$, which is smaller when the bias, $a_1^\top \Gamma \Sigma_{u|t}^{-1/2} \mu_{u|\Delta t}$, is large.

While we have focused on two estimands with the same exposure contrast and different outcomes, similar intuition holds for two estimands with the same outcome and different exposure contrasts. If two estimands have different treatment contrasts, then they will have different values of the $\Sigma_{u|t}^{-1/2} \mu_{u|\Delta t}$ term in their respective biases, and the inner product between these vectors dictates the strength of dependence in the partial identification region. We don't explicitly write down these partial identification regions, as they can be seen as special cases of the partial identification regions we derive later in Section 5.3 that hold in more general settings for any number of estimands.

To take full advantage of the benefits of characterizing the joint partial identification region, we can make additional useful assumptions that can be used to reduce the partial identification regions for all estimands. In the following, we discuss several different kinds of such assumptions.

5.1 Sensitivity Bounds on treatment effects

In many applications, prior knowledge on a reasonable range of effect sizes is known and can be incorporated into the partial identification regions. For instance, in our application to air pollution (Section 7), we know that it is biologically implausible for pollution to have strong protective effects on health outcomes. We may also have strong prior knowledge about the largest plausible harmful effect, as it is not expected for air pollution to be the sole driver of complex public health outcomes. In our notation, a direct assumption about the magnitude of the causal effect on a single estimand takes the form

$$z_l \leq E[a^\top Y(t_1) - a^\top Y(t_2)] \leq z_u,$$

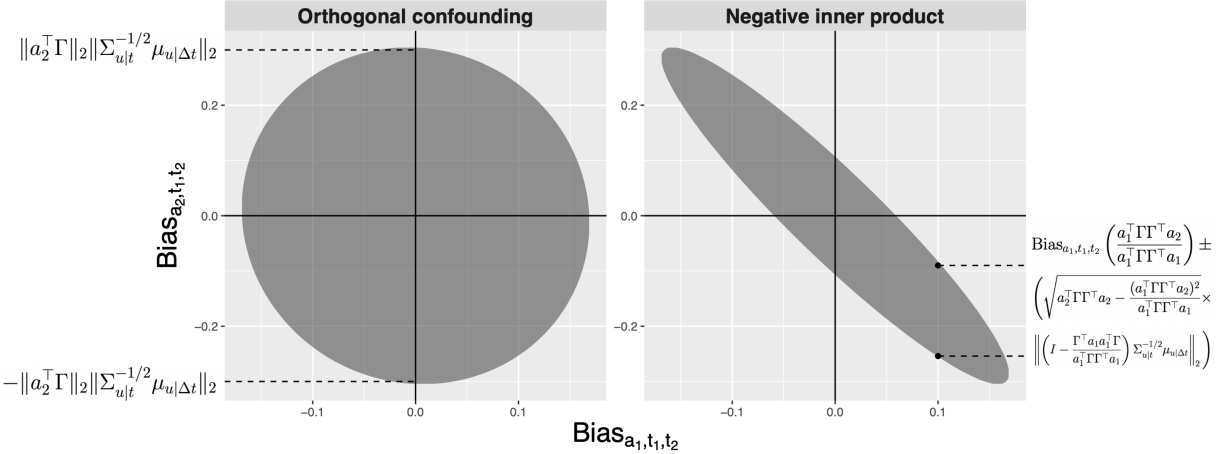


Figure 1: Comparison of bivariate partial identification regions for the bias when either $\langle a_1^\top \Gamma, a_2^\top \Gamma \rangle = 0$ or $\langle a_1^\top \Gamma, a_2^\top \Gamma \rangle < 0$. The horizontal dashed lines in the left panel correspond to the marginal partial identification region for the bias of the second estimand. The horizontal dashed lines in the right panel correspond to the conditional partial identification region for the bias of the second estimand for a particular choice of the bias of the first estimand.

for a given choice of upper and lower bounds on the treatment effect, z_l and z_u . These bounds provide information on the rotation matrix, R , via the following inequality:

$$z_l \leq [a^\top \check{g}(t_1) - a^\top \check{g}(t_2)] - a^\top \tilde{\Gamma} R \Sigma_{u|t}^{-1/2} \mu_{u|\Delta t} \leq z_u. \quad (13)$$

If we make these assumptions for a number of estimands, we gain more information about R , and hence the bias for all other estimands. Analytic characterizations of the partial identification region under these constraints is a non-trivial problem and as such, we find approximate solutions using a rejection sampling algorithm to explore the range of possible causal effects satisfying (13). Specifically, we draw orthogonal matrices $R^{(h)}$ for $h = 1, \dots, H$ uniformly on the Stiefel manifold of $m \times m$ orthogonal matrices, for large values of H . For each orthogonal matrix, $R^{(h)}$, we check whether the constraints in (13) are satisfied. Each matrix $R^{(h)}$ that satisfies the aforementioned criteria determines the bias for each estimand of interest, and we can explore the set of these matrices to determine plausible biases, and therefore partial identification regions. Since m is generally small (e.g., single a digit value), such a Monte Carlo rejection sampling strategy is feasible.

5.2 Sensitivity Bounds on Partial R-squared Values

As an alternative to specifying sensitivity bounds directly on the treatment effects, we can instead specify bounds on the partial variance explained by confounders. In a single-treatment single-outcome analysis, Cinelli and Hazlett (2020) propose specifying upper bounds on both the partial fraction of outcome variance explained by confounders ($R_{Y \sim U|T}^2$) and the fraction of treatment variance explained by confounders ($R_{T \sim U}^2$). Here, we show how their approach can be incorporated into our multi-treatment multi-outcome setting. Throughout this section, we let $d = (t_1 - t_2)$ correspond to the treatment contrast of interest.

For a given treatment-outcome pair, $a^\top Y$ and $d^\top T$, let $U_{a,d}$ represent a scalar projection of U which captures all confounding for that treatment-outcome pair. We call $U_{a,d}$ a “minimal deconfounder” for treatment-outcome pair $a^\top Y$ and $d^\top T$ since it is the lowest dimensional function of U that

is sufficient to address confounding (D'Amour and Franks, 2021). There is no unique minimal deconfounder: for example, both $d^\top B U$ and $a^\top \Gamma \Sigma_{y|t}^{-1/2} U$ are different scalar summaries of U that are sufficient to remove all confounding bias. Despite this, we can still reason about the partial variances explained by such a minimal deconfounder. Here, we consider the fraction of outcome variance explained by the minimal deconfounder given the treatment, $R_{a^\top Y \sim U_{a,d}|T}^2$, and the fraction of treatment variance explained by the minimal deconfounder, $R_{d^\top T \sim U_{a,d}}^2$. These are the sensitivity parameters one would specify in a “one-at-a-time” sensitivity analysis, e.g., using the R-squared style sensitivity analysis proposed by Cinelli and Hazlett (2020). Here, we can rewrite the bias for a given estimand in terms of the partial R-squared values on a minimal sufficient confounder as

$$\text{Bias}_{a,t_1,t_2}^2 = R_{a^\top Y \sim U_{a,d}|T}^2 \frac{R_{d^\top T \sim U_{a,d}}^2}{1 - R_{d^\top T \sim U_{a,d}}^2} \frac{a^\top \Sigma_{y|t} a}{d^\top \Sigma_t d}.$$

Thus, bounds on $R_{a^\top Y \sim U_{a,d}|T}^2$ and $R_{d^\top T \sim U_{a,d}}^2$ imply bounds on the omitted variable bias. Additionally, the factor confounding assumption implies bounds on these partial R^2 values:

$$R_{a^\top Y \sim U_{a,d}|T}^2 \leq \frac{a^\top \Gamma \Gamma^\top a}{a^\top \Sigma_{y|t} a}, \quad R_{d^\top T \sim U_{a,d}}^2 \leq \frac{d^\top B B^\top d}{d^\top \Sigma_t d}. \quad (14)$$

These upper bounds, when they are achieved, correspond to the worst-case bias bound in Theorem 1. One advantage of the multi-treatment, multi-outcome setting with factor confounding is that these upper bounds are identifiable from the observed data. Other approaches, such as the extreme robustness value approach proposed by Cinelli and Hazlett (2020), consider the implications for inference when the partial correlation between the unmeasured confounder and outcome is one (e.g., $R_{a^\top Y \sim U_{a,d}|T}^2 = 1$). In our setting, when we infer $\frac{a^\top \Gamma \Gamma^\top a}{a^\top \Sigma_{y|t} a} \ll 1$, we produce a much less conservative characterization of the range of plausible causal effects.

In practice, it may be reasonable to assume that the minimal sufficient confounder explains an even smaller fraction of the variability in the treatment and outcome than those in (14). Commonly, calibration for these R-squared variables is done by leveraging observed covariates to compute similar benchmark R-squared values. With benchmark values in hand, one could provide bounds on the bias of the causal effect, since the bias of our estimand can be written in terms of these parameters. Finally, as with bounding the treatment effects directly, joint R-squared style sensitivity analysis for multiple estimands can have large benefits relative to a one-at-a-time sensitivity analysis. The partial R-squared values for each estimand are not variationally independent, as they depend on the common rotation matrix parameter R , and thus if we require marginal bounds to be satisfied concurrently for all estimands, then the implied joint bounds for individual estimands can be much tighter. To find the partial identification regions, we can use the same sampling algorithm discussed in Section 5.1, where we retain rotation matrices that satisfy all of the partial R-squared constraints.

5.3 Negative controls

Negative controls have been widely used in observational studies to detect or mitigate bias in the causal effect of the treatment on the outcome. In air pollution epidemiology, examples include future air pollutant levels or air pollutant levels in a distant area being used as negative control exposures (Lumley and Sheppard, 2000), and appendicitis hospitalizations being used as a negative

control outcome (Sheppard et al., 1999). Generally, in the multi-treatment, multi-outcome setting, we refer to a negative control pair as any treatment and outcome pair among our k treatments and q outcomes for which we assume *a priori* that the PATE for that treatment-outcome pair is zero. Such negative control assumptions can be viewed as a special case of a sensitivity bound on the treatment effects described in Section 5.1, where the constraints in (13) are set so that $z_l = z_u = 0$. Given the importance of null controls in the literature, we elaborate on this special case below.

Suppose throughout that we have J outcomes with at least one treatment known to not causally affect that outcome, and that the j th outcome has $c_j \leq m$ such negative control pairs. The j th outcome is denoted by $b_j^\top Y$, and the treatment contrasts for outcome j are given by

$$\left\{ \left(t_1^{(j,1)}, t_2^{(j,1)} \right), \dots, \left(t_1^{(j,c_j)}, t_2^{(j,c_j)} \right) \right\}.$$

We further define the difference in the $\check{g}(\cdot)$ function at these contrasts as

$$\check{\mathcal{G}}_j = \left[\check{g}\left(t_1^{(j,1)}\right) - \check{g}\left(t_2^{(j,1)}\right), \dots, \check{g}\left(t_1^{(j,c_j)}\right) - \check{g}\left(t_2^{(j,c_j)}\right) \right]. \quad (15)$$

Negative controls provide information on the rotation matrix R through the following equation:

$$b_j^\top \tilde{\Gamma} R M_j = b_j^\top \check{\mathcal{G}}_j, \quad (16)$$

where

$$M_j = \Sigma_{u|t}^{-1/2} \left[\mu_{u|t_1^{(j,1)}} - \mu_{u|t_2^{(j,1)}}, \dots, \mu_{u|t_1^{(j,c_j)}} - \mu_{u|t_2^{(j,c_j)}} \right]. \quad (17)$$

The left side of (16) is the functional form for the bias of negative control estimands, while the right side corresponds to the estimated causal effects under “no unobserved confounding”. For null controls, these are equal by definition since the true causal estimand is assumed to be zero *a priori*. This equation restricts the space of possible R matrices, and therefore can reduce the size of the partial identification region for all estimands of interest.

The partial identification regions with null control constraints can be complex, even consisting of either disjoint intervals or isolated points. Below, we introduce a constrained optimization problem for deriving these partial identification regions under arbitrary negative control constraints, and derive analytic partial identification regions that are conservative at times, but provide intuition about the benefits of negative controls.

5.3.1 Approaches to finding negative control partial identification regions

For any feasible omitted variable bias, β , with $|\beta| \leq \|a^\top \Gamma\|_2 \|\Sigma_{u|t}^{-1/2} \mu_{u|\Delta t}\|_2$, to be consistent with the negative control assumption in (16), there must be an orthogonal matrix R such that the following conditions are satisfied:

1. $a^\top \tilde{\Gamma} R \Sigma_{u|t}^{-1/2} \mu_{u|\Delta t} = \beta$.
2. $b_j^\top \tilde{\Gamma} R M_j = b_j^\top \check{\mathcal{G}}_j$ for all $j = 1, \dots, J$ negative control contrasts.

The first condition establishes that for rotation matrix R the omitted variable bias for outcome $a^\top Y$ is indeed β . The other conditions ensure that the orthogonal matrix R also implies the correct omitted variable biases for the negative controls. For certain values of β , there may not exist a

matrix R that satisfies the null control conditions. We can express the partial identification region for Bias_{a,t_1,t_2} as the set $\mathcal{B}_{a,t_1,t_2} = \{\beta : \nu_\beta = 0\}$ where

$$\nu_\beta := \min_{\tilde{R} \in \mathcal{V}_{m,m}} \left((a^\top \tilde{\Gamma} \tilde{R} \Sigma_{u|t}^{-1/2} \mu_{u|\Delta t} - \beta)^2 + \sum_{j=1}^J \|b_j^\top \tilde{\Gamma} \tilde{R} M_j - b_j^\top \check{\mathcal{G}}_j\|_2^2 \right), \quad (18)$$

and $\mathcal{V}_{m,m}$ is the Stiefel manifold of all $m \times m$ orthogonal matrices. If the bias value β is in the partial identification region established by the negative control constraints, then $\nu_\beta = 0$. Therefore, for any β , we minimize equation (18) over the Stiefel manifold using the optimization algorithm implemented in the `rstiefel` package (Hoff and Franks, 2019). To find the partial identification region, we minimize (18) over a grid of all possible values of β and keep track of those that minimize this objective function at zero. In practice, the numerical solutions ν_β are never exactly zero, and thus we simply check that both $(a_1^\top \tilde{\Gamma} \tilde{R} \Sigma_{u|t}^{-1/2} \mu_{u|\Delta t} - \beta)^2 \leq \delta_1$ and $\sum_{j=1}^J \|b_j^\top \tilde{\Gamma} \tilde{R} M_j - b_j^\top \check{\mathcal{G}}_j\|_2^2 \leq \delta_2$ for sufficiently small constants $\delta_1, \delta_2 > 0$. A full description of the algorithm for identifying feasible biases can be found in Appendix B.

In addition to finding the bounds computationally, we are able to derive partial identification regions analytically. While these regions can be conservative in certain situations, they provide useful insight into the types of negative controls that lead to the largest reduction in the size of the partial identification region.

Theorem 3. *Suppose we only have $J = 1$ negative control outcome with $c_1 \leq m$ negative control contrasts and that Assumptions 1–4 hold. Let $k_{aa} = a^\top \Gamma \Gamma^\top a$, $k_{ab} = a^\top \Gamma \Gamma^\top b_1$, and $k_{bb} = b_1^\top \Gamma \Gamma^\top b_1$, which are all identifiable scalars from our factor model assumptions. Lastly, let M_1^\dagger be a generalized inverse of M_1 . Then, Bias_{a,t_1,t_2} is in the following interval*

$$\frac{k_{ab}}{k_{bb}} b_1^\top \check{\mathcal{G}}_1 M_1^\dagger \Sigma_{u|t}^{-1/2} \mu_{u|\Delta t} \pm \left(\left| \frac{k_{ab}}{k_{bb}} \right| \sqrt{k_{bb} - \|b_1^\top \check{\mathcal{G}}_1 M_1^\dagger\|_2^2} \| (I - M_1 M_1^\dagger) \Sigma_{u|t}^{-1/2} \mu_{u|\Delta t} \|_2 + \sqrt{k_{aa} - \frac{k_{ab}^2}{k_{bb}}} \|\Sigma_{u|t}^{-1/2} \mu_{u|\Delta t}\|_2 \right), \quad (19)$$

The proof of Theorem 3 can be seen in Appendix A. This result shows that negative controls provide the largest benefit when (i) $a^\top \Gamma \Gamma^\top b_1$ is large in magnitude, (ii) the confounding bias of the negative control given by $b_1^\top \check{\mathcal{G}}_j$ is large, and (iii) when M_1^\dagger is colinear with $\Sigma_{u|t}^{-1/2} \mu_{u|\Delta t}$. The first condition occurs when the negative control outcome and the outcome of interest have similar confounding mechanisms, meaning that the same linear combinations of the unmeasured confounders affect their outcomes. The second condition simply implies that the negative control estimand also suffers from bias due to the unmeasured confounders. The third condition occurs when the linear combinations of the unmeasured confounders that affect both the negative control treatment and the treatment of interest are similar. Therefore, ideal negative control pairs are those with large confounding biases and similar confounding mechanisms as the estimand of interest. While we focused on $J = 1$ in Theorem 3 to build intuition, we extend this result to settings with $J > 1$ in Appendix A.

5.3.2 Identification conditions with negative controls

While the focus of our paper is generally on partial identification, we show here that under certain scenarios, negative controls can point identify the causal effect of interest. This further shows the potential benefit of negative controls and provides connections between our work and identification

scenarios in the literature on double negative controls (Miao et al., 2018; Shi et al., 2020a,b; Hu et al., 2023).

Theorem 4. *Suppose we have J negative control outcomes and define $b = [b_1, b_2, \dots, b_J]$ to be a $q \times J$ matrix that has each individual b_j as its columns. Let b^* be a $q \times J^*$ matrix comprising of a subset of the columns in b where $1 \leq J^* \leq J$, and define \mathcal{J}^* to be the set of indices for the columns of b that make up b^* . Additionally, let $\mathcal{C}(A)$ represent the column space of a matrix A . Under the assumptions and conditions of Theorem 3, the causal effect is identifiable under any of the following scenarios.*

1. $a^\top \Gamma \in \mathcal{C}(\Gamma^\top b^*)$ and $b_j^\top \Gamma \in \mathcal{C}(M_j)$ for all $j \in \mathcal{J}^*$
2. There exists a j such that $a^\top \Gamma$ is colinear with $b_j^\top \Gamma$ and $\Sigma_{u|t}^{-1/2} \mu_{u|\Delta t} \in \mathcal{C}(M_j)$.
3. $\Sigma_{u|t}^{-1/2} \mu_{u|\Delta t} \in \mathcal{C}(\Gamma^\top b^*)$ and $b_j^\top \Gamma \in \mathcal{C}(M_j)$ for all $j \in \mathcal{J}^*$

A proof of this result can be found in Appendix A. While these conditions may seem abstract, they do hold in some plausible scenarios. For example, scenario 1 holds automatically when we have m negative control exposures, i.e., negative control pairs with the same outcome as the estimand of interest, but different exposure contrasts. Identification can also be obtained if additional assumptions are made, such as the existence of a so-called confounding bridge function (Miao et al., 2018), though we point readers to the literature on double negative controls for a discussion of such assumptions. Lastly, it is important to emphasize that within our framework, negative controls are still useful even if these conditions do not hold, as they can reduce the widths of the partial identification region substantially compared with the widths without negative controls. This is related to recent work on partial identification in the proximal causal inference literature where partial identification can be obtained when assumptions required for point identification do not hold (Ghassami et al., 2023).

6 Simulation study

Here, we present a brief simulation study to highlight the benefits of characterizing the joint partial identification region for multiple estimands. For simplicity, we focus on a single data set with sample size $n = 10^6$ to effectively eliminate sampling variability and focus on the uncertainty caused by the potential presence of unmeasured confounders. For brevity, we leave explicit details of the data generation process to Appendix D. To summarize, we consider a problem with $k = 10$ exposures and $q = 6$ outcomes, with $m = 3$ unmeasured confounders. The true effect sizes for all estimands are between -1 and 1 , and there are a number of treatments with no effect on specific outcomes, leading to multiple potential negative controls. We use linear models throughout, which contains the true data generating mechanism, though similar results hold for more complex estimators of $g(\cdot)$. Our inferential goal is to estimate the effect of a particular exposure on a single outcome. We scaled the confounding and effect sizes so that the estimate obtained assuming no unmeasured confounding is 0, while the true value of the estimand is 1. To illustrate the different assumptions or constraints that one can place, we derive the partial identification region for this estimand under a variety of different assumptions, summarized below.

1. Bounds in equation (7) that rely only on the factor confounding structure (Factor confounding)
2. Incorporating a single negative control outcome (Negative control outcome)

3. Incorporating a negative control for which the treatment and outcome for the negative control are both different from the estimand of interest (Negative control pair)
4. Incorporating two negative control outcomes simultaneously (Two negative control outcomes)
5. Effect size constraints as in Section 5.1 with $z_l = -1.2$ and $z_u = 1.2$. Constraints are simultaneously placed on the effect of the exposure of interest on the five outcomes that are not of interest. (Effect size < 1.2)
6. The same effect size constraints, but with $z_l = -2$ and $z_u = 2$ (Effect size < 2)
7. Partial R-squared constraints as in Section 5.2 placed on the same estimands as for the effect size constraints with $R_{d^\top T \sim U_{a,d}}^2 \leq 0.35$ and $R_{a^\top Y \sim U_{a,d}|T}^2 \leq 0.15$. (R-squared < 0.15)
8. The same partial R-squared constraints, but with $R_{a^\top Y \sim U_{a,d}|T}^2 \leq 0.25$ (R-squared < 0.25)

The results can be found in Figure 2, where we see that all partial identification regions contain the true value of the estimand, though different constraints lead to very different partial identification regions. In terms of negative controls, we see in this case that the negative control pair, which looks at a completely distinct treatment and outcome from the estimand of interest, is still very informative for the estimand of interest, as they have similar confounding mechanisms. Having two negative control exposures is also very informative, and in this case leads to disjoint regions. The effect size constraints are extremely powerful in this case, even for the more relaxed constraint using 2 as a cutoff value, as the region is very small and contains the true value. Interestingly, for small enough partial R-squared constraints we can obtain disjoint intervals as seen by the interval using a cutoff of 0.15. This is because it is not possible for all partial R-squared values to be zero as they all depend on the shared R matrix. As these constraints are weakened to a cutoff of 0.25, this disappears and we obtain a single, wider interval.

Overall, these results show that different constraints or assumptions can be more or less informative about the estimand of interest depending on the situation. Further, it shows that using no constraints (factor confounding only) can lead to very wide, uninformative intervals, but reasonable additional constraints result in far more informative intervals, which in this case are correctly able to rule out a causal effect of zero, despite zero being the estimate obtained assuming no unmeasured confounding. This highlights that the approaches developed here need not be centered around the estimate obtained with no unmeasured confounding, and that the partial identification regions are able to provide tight bounds around the true value, even under a large amount of confounding bias.

7 Estimating the health effects of components of PM_{2.5}

Now we return to the motivating example and data analysis, which was introduced in Section 2. We standardize all exposures and outcomes to have mean zero and standard deviation one prior to running the analysis so that the effect estimates are all on the same scale across outcomes and exposure combinations. For example, an estimate of 0.1 for a particular shift in exposures would be interpreted as being expected to change the outcome by 0.1 outcome standard deviations. The estimands we look at are the effects of shifting one exposure from their 1st to 3rd quartile, while holding the remaining exposures fixed at their median value. We estimate $g(\cdot)$ and therefore the effects of the exposures (and confounders) on the outcome using a linear regression model, and use the aforementioned approaches to assess the robustness of these estimates to unmeasured confounding bias. For more details on the estimation of all model parameters, including factor

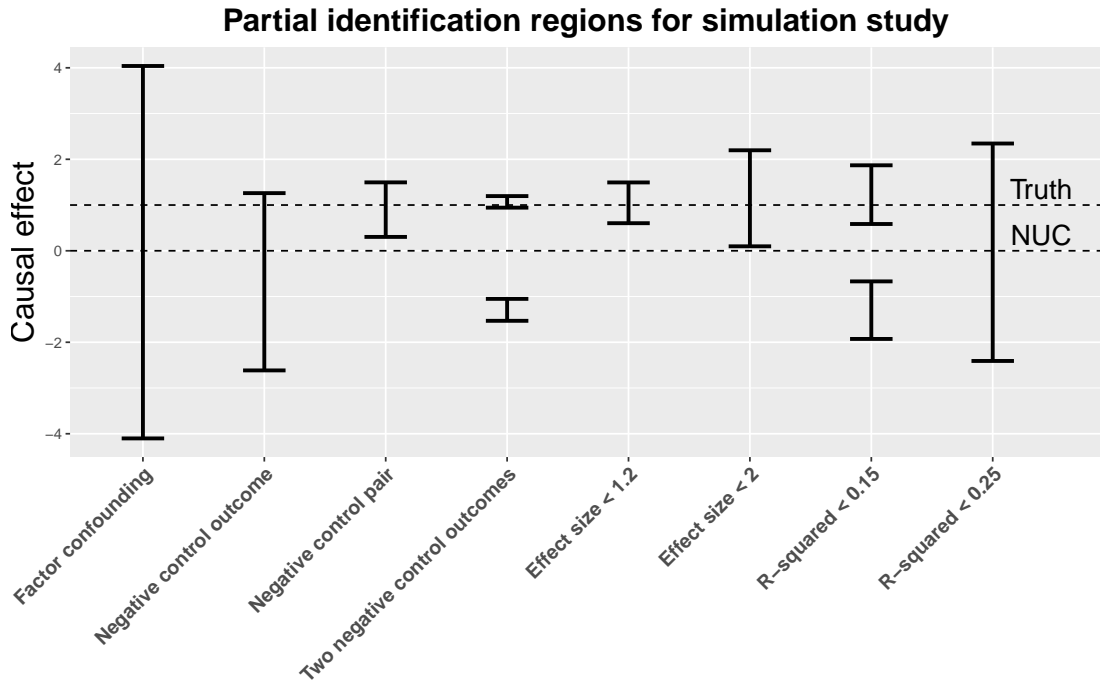


Figure 2: Partial identification regions under different constraints in simulated data set. The true value is represented by the dotted line at 1, while the estimate obtained assuming no unmeasured confounding (NUC) is represented by the dotted line at 0.

model parameters, see Appendix C.

We also note that the factor confounding assumption (Assumption 4) is plausible in this application. All outcomes correspond to hospitalization rates for different diseases, and it is reasonable that certain characteristics, which are not measured in our observed covariates, are broadly associated with poor health outcomes. For instance, these unmeasured characteristics likely reflect features like health-seeking behavior or proximity to and/or quality of health care access. Similarly, exposures tend to be elevated in areas with various pollutant emitting sources such as roadways, power plants, and factories. Certain communities are more likely to be near these sources of pollution due to underlying structural inequalities, which again points to the plausibility of the shared confounding mechanism.

7.1 Factor loadings and implications for unmeasured confounding

Estimates of the factor model parameters are shown in Figure 3. The maximum number of factors that can be identified in factor analysis with 6 exposures and 6 outcomes (including the negative control outcome) is $m = 3$ for both treatment and outcome models. We proceed with $m = 3$ for this reason, as it will provide the most conservative inferences about causal effects of interest. We see that there are many large factor loadings, particularly in the exposure loading matrix, B . However, we find that ozone has very small factor loadings, indicating little dependence with the other exposures. The first column of the outcome loading matrix, Γ , largely reflects correlation among pulmonary outcomes: COPD, lung cancer and prior COPD. As such, prior COPD is an especially useful null control outcome for COPD and lung cancer. The factor loadings also provide

information about $R_{a^\top Y \sim U|T,X}^2$ and $R_{d^\top T \sim U|X}^2$ for each outcome, a , and exposure, d (see Table 1). Larger values of these R-squared values imply wider partial identification regions for those exposures or outcomes due to the increased potential for unmeasured confounding bias.

Table 1: Partial R-squared values between unmeasured variables and each of the exposures and outcomes

	Anemia	COPD	Stroke	Lung cancer	Asthma	Prior COPD
$R_{a^\top Y \sim U T,X}^2$	0.247	0.976	0.048	0.076	0.138	0.268
	Ammonium	Ozone	Elemental carbon	Nitrates	Organic carbon	Sulfates
$R_{d^\top T \sim U X}^2$	0.985	0.023	0.99	0.788	0.434	0.824

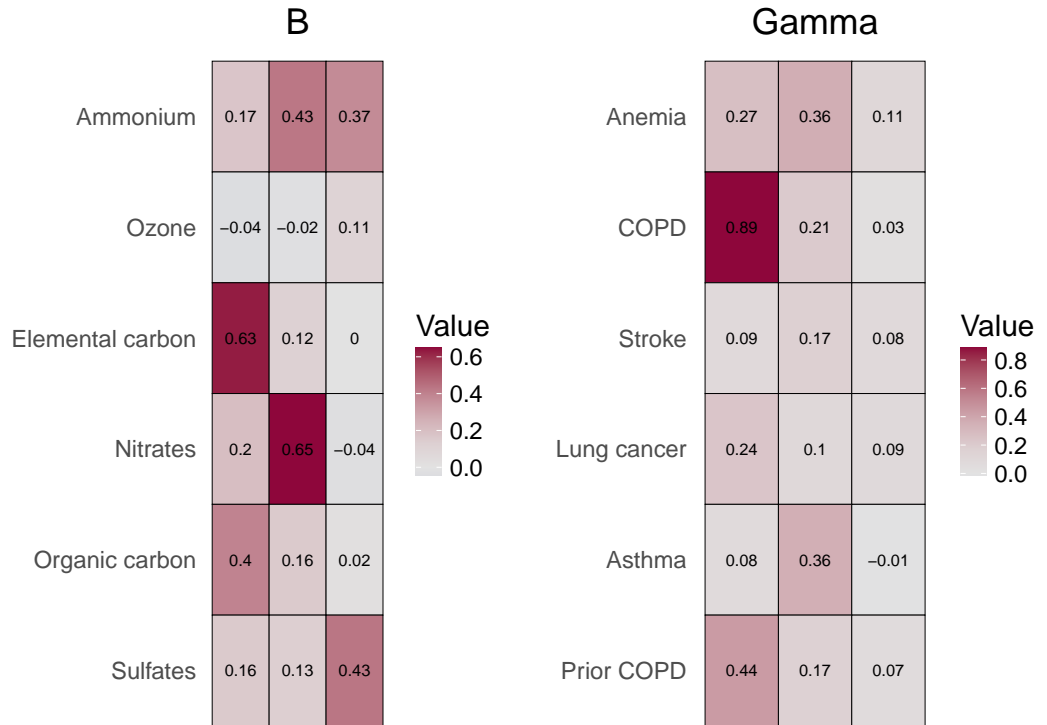


Figure 3: Estimates of the B and Γ matrices.

7.2 Causal effect of organic carbon and nitrates

We now explore the partial identification regions for the effect of both organic carbon and nitrates on the outcomes of interest. We focus on these two exposures in the manuscript for simplicity, and because these two exposures illustrate two distinct scenarios where either the partial identification regions are informative about the causal effect, or they are not informative. The results for other exposures are included in Appendix E. The partial identification regions for the other exposures generally contain zero and are wide for elemental carbon, sulfates, and ammonium due to the large partial R-squared values seen in Table 1. We incorporate two different constraints when calculating the partial identification regions for each exposure of interest: 1) using prior COPD as a negative control outcome, and 2) using prior COPD as a negative control outcome and placing an effect size constraint on the effect of that exposure on asthma hospitalizations with $z_l = -0.05$

and $z_u = 0.2$. The lower bound stems from prior research and biologic implausibility of pollution having a protective effect on health, while the upper bound is based on prior literature looking at larger shifts in particulate matter than those considered here, which have estimated smaller effects than this upper bound (Di et al., 2017). Complex public health outcomes such as hospitalization rates are driven by a host of factors (smoking and obesity, among others), and particulate matter only explains a small part of the variability in these outcomes. Given that our outcomes are standardized, it is therefore implausible to have an effect size of 0.25 or 0.5 as this would imply that pollution explains a large portion of the variability in hospitalization rates. To ensure that any results we see are not strictly due to the asymmetric nature of our bound, we apply symmetric bounds in Appendix E and find similar conclusions.

The results for both exposures can be found in Figure 4. The partial identification regions for the effect of organic carbon on both COPD and stroke lie entirely above zero showing robust evidence of a detrimental causal effect of organic carbon on these two outcomes. The intervals are generally wider and less informative for nitrates, likely due to the larger value of $R^2_{d^\top T \sim U}$ for this exposure. Another interesting finding here is that the point estimates under no unmeasured confounding for organic carbon are sometimes not contained in the partial identification region, and can even be of the opposite sign as the partial identification region, particularly for the effect of organic carbon on COPD. This shows the importance of accounting for the potential presence of unmeasured confounding in this context, as different conclusions are obtained once we account for the possibility of unmeasured confounding.

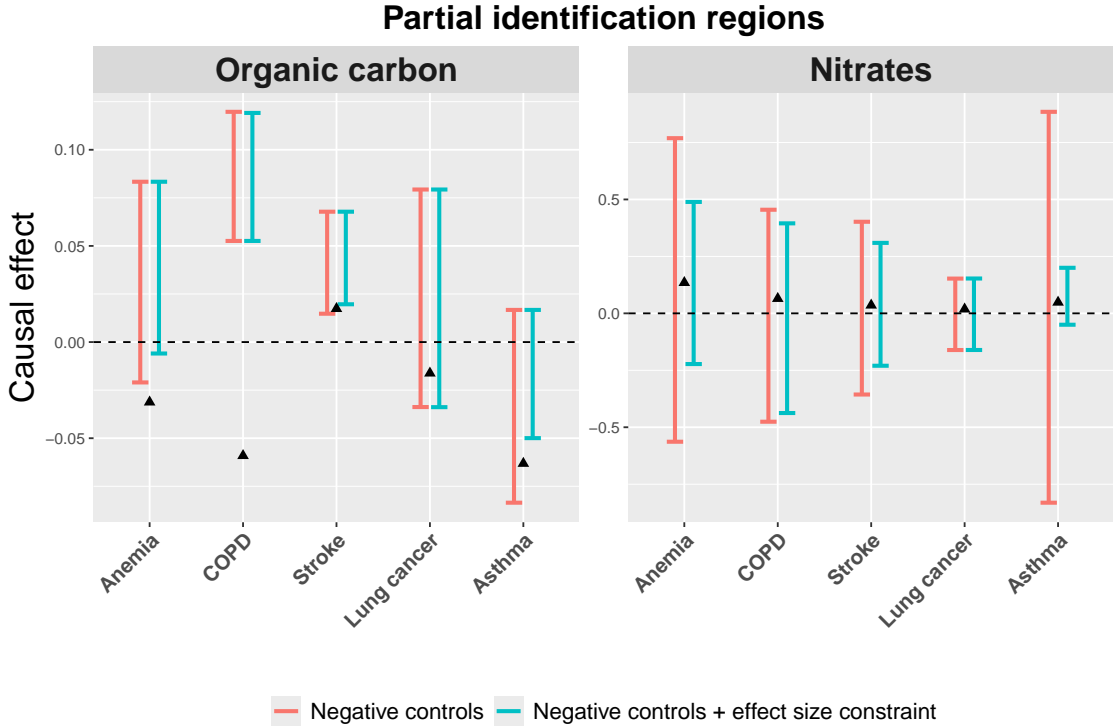


Figure 4: Partial identification regions for the causal effect of organic carbon and nitrates under both a negative control and effect size constraint. The triangles represent the estimates obtained assuming no unmeasured confounding.

More refined information about the plausible values of these causal effects can be seen by examining bivariate partial identification regions. For example, in the left panel of Figure 5, we see that the lower bound for the effect of organic carbon on COPD rates can be sharpened depending on one's belief of the effect of organic carbon on anemia. If one assumes there is no effect of organic carbon on anemia, then the effect on COPD is nearly 0.1, larger than the lower bound seen in the univariate region for the effect of organic carbon on COPD rates. The minimum value of the effect of organic carbon on COPD is only obtained if there is a large effect of organic carbon on anemia as well. This suggests that there is either a very large effect of organic carbon on COPD rates, or there is a moderate effect of organic carbon on both COPD and anemia rates. The right panel provides interesting information about the effect of organic carbon on anemia. While the univariate bound in Figure 4 contained zero for the effect of organic carbon on anemia, the bivariate plot shows that this effect can only be zero if there is a large, protective effect of organic carbon on asthma. Given that it is unexpected for organic carbon to reduce asthma rates, this suggests a likely effect of organic carbon on anemia as well. Similar to the univariate setting, we see that the estimates obtained under no unmeasured confounding are not contained in the partial identification region, and would lead to drastically different conclusions. Overall, this analysis provides strong, robust evidence of a causal effect of organic carbon on public health outcomes.

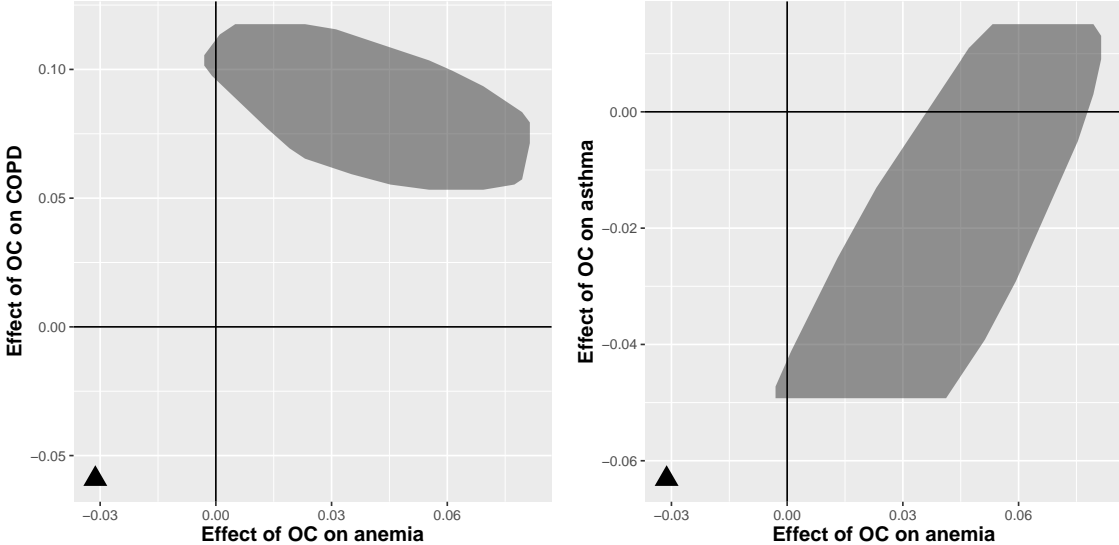


Figure 5: Bivariate partial identification regions after both negative control and effect size constraints have been incorporated. The left panel shows the effect of organic carbon on both anemia and COPD rates. The right panel shows the effect of organic carbon on both anemia and asthma rates. The triangles represent the point estimates under no unmeasured confounding.

8 Discussion

In this paper, we develop a framework for identifying partial identification regions in the presence of unmeasured confounding when the data contain multiple treatments and multiple outcomes, which is particularly useful for studying the health effects of multivariate air pollutants. We illustrate how a factor confounding assumption can be leveraged to learn more about the range of plausible causal effects across multiple estimands. For one, we obtain bounds on causal effects that are identifiable from the observed data alone. These partial identification regions can be reduced in size significantly

under reasonable constraints that are known a priori given subject-matter expertise, which one typically has in environmental studies. One of the constraints we consider are negative control assumptions, for which we develop theory and algorithms to produce refined partial identification regions. Alternatively, prior knowledge on plausible effect sizes or constraints on partial R^2 values obtained through calibration to observed covariates, can be used to provide more informative partial identification regions. Overall, our theoretical and empirical studies suggest that the proposed framework yields new insights about causal effects even in the presence of unmeasured confounding variables. This was evident in a nationwide analysis of the effects of particulate matter components on cause specific hospitalizations using Medicare claims data, which showed a strong, harmful effect of organic carbon on public health outcomes.

There are a number of potentially interesting future research directions that could expand upon this work and make partial identification in multi-treatment and multi-outcome settings more widely applicable. For one, we have focused on continuous treatments here, which facilitates the use of the factor models used throughout, but extending these ideas to categorical treatments and generalized linear models would be an important extension of this work. Related, our current framework relies on the factor confounding assumption, and it would be useful to study the robustness of our findings to violations of this assumption. Lastly, we studied the refinement of the partial identification region in the presence of negative controls or prior constraints on effect sizes and R^2 values, but other a priori assumptions, such as sparsity of treatment effects, could be incorporated as well. Extending our work to these other situations would be a natural extension that could broaden the scope of this work.

Acknowledgements

Research described in this article was conducted under contract to the Health Effects Institute (HEI), an organization jointly funded by the United States Environmental Protection Agency (EPA) (Assistance Award No. CR-83590201) and certain motor vehicle and engine manufacturers. The contents of this article do not necessarily reflect the views of HEI, or its sponsors, nor do they necessarily reflect the views and policies of the EPA or motor vehicle and engine manufacturers. The computations in this paper were run on the FASRC Cannon/FASSE cluster supported by the FAS Division of Science Research Computing Group at Harvard University.

References

Anderson, T. and Rubin, H. (1956). Statistical inference in. In *Proceedings of the Third Berkeley Symposium on Mathematical Statistics and Probability: Held at the Statistical Laboratory, University of California, December, 1954, July and August, 1955*, volume 1, page 111. Univ of California Press.

Burnett, R., Chen, H., Szyszkowicz, M., Fann, N., Hubbell, B., Pope III, C. A., Apte, J. S., Brauer, M., Cohen, A., Weichenthal, S., et al. (2018). Global estimates of mortality associated with long-term exposure to outdoor fine particulate matter. *Proceedings of the National Academy of Sciences*, 115(38):9592–9597.

Carone, M., Dominici, F., and Sheppard, L. (2020). In pursuit of evidence in air pollution epidemiology: the role of causally driven data science. *Epidemiology (Cambridge, Mass.)*, 31(1):1.

Chernozhukov, V., Cinelli, C., Newey, W., Sharma, A., and Syrgkanis, V. (2022). Long story short:

Omitted variable bias in causal machine learning. Technical report, National Bureau of Economic Research.

Cinelli, C. and Hazlett, C. (2020). Making sense of sensitivity: Extending omitted variable bias. *Journal of the Royal Statistical Society Series B-Statistical Methodology*, 82(1):39–67.

Cohen, A. J., Brauer, M., Burnett, R., Anderson, H. R., Frostad, J., Estep, K., Balakrishnan, K., Brunekreef, B., Dandona, L., Dandona, R., et al. (2017). Estimates and 25-year trends of the global burden of disease attributable to ambient air pollution: an analysis of data from the global burden of diseases study 2015. *The lancet*, 389(10082):1907–1918.

Cornfield, J., Haenszel, W., Hammond, E. C., Lilienfeld, A. M., Shimkin, M. B., and Wynder, E. L. (1959). Smoking and lung cancer: recent evidence and a discussion of some questions. *Journal of the National Cancer institute*, 22(1):173–203.

D'Amour, A. and Franks, A. (2021). Deconfounding scores: Feature representations for causal effect estimation with weak overlap. *arXiv preprint arXiv:2104.05762*.

Di, Q., Wang, Y., Zanobetti, A., Wang, Y., Koutrakis, P., Choirat, C., Dominici, F., and Schwartz, J. D. (2017). Air pollution and mortality in the medicare population. *New England Journal of Medicine*, 376(26):2513–2522.

Di, Q., Wei, Y., Shtein, A., Hultquist, C., Xing, X., Amini, H., Shi, L., Kloog, I., Silvern, R., Kelly, J., et al. (2021). Daily and annual pm2. 5 concentrations for the contiguous united states, 1-km grids, v1 (2000-2016). *NASA Socioeconomic Data and Applications Center (SEDAC)*.

Ding, P. and VanderWeele, T. J. (2016). Sensitivity analysis without assumptions. *Epidemiology (Cambridge, Mass.)*, 27(3):368.

Dominici, F. and Zigler, C. (2017). Best practices for gauging evidence of causality in air pollution epidemiology. *American journal of epidemiology*, 186(12):1303–1309.

Freidling, T. and Zhao, Q. (2022). Sensitivity analysis with the r^2 -calculus. *arXiv preprint arXiv:2301.00040*.

Ghassami, A., Shpitser, I., and Tchetgen, E. T. (2023). Partial identification of causal effects using proxy variables. *arXiv preprint arXiv:2304.04374*.

Hoff, P. and Franks, A. (2019). *rstiefel: Random Orthonormal Matrix Generation and Optimization on the Stiefel Manifold*. R package version 1.0.0.

Hu, J. K., Zorzetto, D., and Dominici, F. (2023). A bayesian nonparametric method to adjust for unmeasured confounding with negative controls. *arXiv preprint arXiv:2309.02631*.

Huang, C., Nichols, C., Liu, Y., Zhang, Y., Liu, X., Gao, S., Li, Z., and Ren, A. (2015). Ambient air pollution and adverse birth outcomes: a natural experiment study. *Population health metrics*, 13:1–7.

Imbens, G. W. (2003). Sensitivity to exogeneity assumptions in program evaluation. *American Economic Review*, 93(2):126–132.

Kong, D., Yang, S., and Wang, L. (2022). Identifiability of causal effects with multiple causes and a binary outcome. *Biometrika*, 109(1):265–272.

Kuroki, M. and Pearl, J. (2014). Measurement bias and effect restoration in causal inference. *Biometrika*, 101(2):423–437.

Luechinger, S. (2014). Air pollution and infant mortality: A natural experiment from power plant desulfurization. *Journal of health economics*, 37:219–231.

Lumley, T. and Sheppard, L. (2000). Assessing seasonal confounding and model selection bias in air pollution epidemiology using positive and negative control analyses. *Environmetrics: The official journal of the International Environmetrics Society*, 11(6):705–717.

Manisalidis, I., Stavropoulou, E., Stavropoulos, A., and Bezirtzoglou, E. (2020). Environmental and health impacts of air pollution: a review. *Frontiers in public health*, 8:14.

Manski, C. F. (1990). Nonparametric bounds on treatment effects. *The American Economic Review*, 80(2):319–323.

McCandless, L. C., Gustafson, P., and Levy, A. (2007). Bayesian sensitivity analysis for unmeasured confounding in observational studies. *Statistics in medicine*, 26(11):2331–2347.

Miao, W., Hu, W., Ogburn, E. L., and Zhou, X.-H. (2022). Identifying effects of multiple treatments in the presence of unmeasured confounding. *Journal of the American Statistical Association*, pages 1–15.

Miao, W., Shi, X., and Tchetgen Tchetgen, E. (2018). A confounding bridge approach for double negative control inference on causal effects. *arXiv preprint arXiv:1808.04945*.

Penrose, R. (1955). A generalized inverse for matrices. In *Mathematical proceedings of the Cambridge philosophical society*, volume 51, pages 406–413. Cambridge University Press.

Portney, P. R. (1990). Policy watch: economics and the clean air act. *Journal of Economic Perspectives*, 4(4):173–181.

Requia, W., Wei, Y., Shtein, A., Hultquist, C., Xing, X., Di, Q., et al. (2021). Daily 8-hour maximum and annual O₃ concentrations for the contiguous United States, 1-km grids, v1 (2000–2016). *NASA Socioeconomic Data and Applications Center (SEDAC)*.

Revelle, W. and Rocklin, T. (1979). Very simple structure: An alternative procedure for estimating the optimal number of interpretable factors. *Multivariate behavioral research*, 14(4):403–414.

Rich, D. Q. (2017). Accountability studies of air pollution and health effects: lessons learned and recommendations for future natural experiment opportunities. *Environment international*, 100:62–78.

Rosenbaum, P. R. (1987). Sensitivity analysis for certain permutation inferences in matched observational studies. *Biometrika*, 74(1):13–26.

Rosenbaum, P. R. (1988). Sensitivity analysis for matching with multiple controls. *Biometrika*, 75(3):577–581.

Rosenbaum, P. R. (1991). Sensitivity analysis for matched case-control studies. *Biometrics*, pages 87–100.

Rosenbaum, P. R. (2002a). Covariance adjustment in randomized experiments and observational studies. *Statistical Science*, 17(3):286–327.

Rosenbaum, P. R. (2002b). *Overt bias in observational studies*. Springer.

Rosenbaum, P. R. and Rubin, D. B. (1983). Assessing sensitivity to an unobserved binary covariate in an observational study with binary outcome. *Journal of the Royal Statistical Society: Series B (Methodological)*, 45(2):212–218.

Rubin, D. B. (1974). Estimating causal effects of treatments in randomized and nonrandomized studies. *Journal of Educational Psychology*, 66(5):688.

Schwartz, J., Wei, Y., Dominici, F., and Yazdi, M. D. (2023). Effects of low-level air pollution exposures on hospital admission for myocardial infarction using multiple causal models. *Environmental Research*, page 116203.

Sheppard, L., Levy, D., Norris, G., Larson, T. V., and Koenig, J. Q. (1999). Effects of ambient air pollution on nonelderly asthma hospital admissions in seattle, washington, 1987–1994. *Epidemiology*, 10(1):23–30.

Shi, X., Miao, W., Nelson, J. C., and Tchetgen Tchetgen, E. J. (2020a). Multiply robust causal inference with double-negative control adjustment for categorical unmeasured confounding. *Journal of the Royal Statistical Society Series B: Statistical Methodology*, 82(2):521–540.

Shi, X., Miao, W., and Tchetgen Tchetgen, E. (2020b). A selective review of negative control methods in epidemiology. *Current epidemiology reports*, 7:190–202.

Small, D. S. (2007). Sensitivity analysis for instrumental variables regression with overidentifying restrictions. *Journal of the American Statistical Association*, 102(479):1049–1058.

Sommer, A. J., Leray, E., Lee, Y., and Bind, M.-A. C. (2021). Assessing environmental epidemiology questions in practice with a causal inference pipeline: An investigation of the air pollution–multiple sclerosis relapses relationship. *Statistics in Medicine*, 40(6):1321–1335.

Splawa-Neyman, J., Dabrowska, D. M., and Speed, T. P. (1990). On the application of probability theory to agricultural experiments. essay on principles. section 9. *Statistical Science*, pages 465–472.

Tchetgen Tchetgen, E. J., Ying, A., Cui, Y., Shi, X., and Miao, W. (2024). An introduction to proximal causal inference. *Statistical Science*, 39(3):375–390.

Van Donkelaar, A., Martin, R. V., Li, C., and Burnett, R. T. (2019). Regional estimates of chemical composition of fine particulate matter using a combined geoscience-statistical method with information from satellites, models, and monitors. *Environmental science & technology*, 53(5):2595–2611.

VanderWeele, T. J. and Ding, P. (2017). Sensitivity analysis in observational research: introducing the e-value. *Annals of internal medicine*, 167(4):268–274.

Veitch, V. and Zaveri, A. (2020). Sense and sensitivity analysis: Simple post-hoc analysis of bias due to unobserved confounding. *Advances in Neural Information Processing Systems*, 33:10999–11009.

Velicer, W. F. (1976). Determining the number of components from the matrix of partial correlations. *Psychometrika*, 41:321–327.

Wang, J., Zhao, Q., Hastie, T., and Owen, A. B. (2017). Confounder adjustment in multiple hypothesis testing. *Annals of statistics*, 45(5):1863.

Wu, Y., Liu, M., Yan, J., Fu, Y., Wang, S., Wang, Y., and Sun, X. (2023). The blessings of multiple treatments and outcomes in treatment effect estimation. *arXiv preprint arXiv:2309.17283*.

Zheng, J., D'Amour, A., and Franks, A. (2021). Copula-based sensitivity analysis for multi-treatment causal inference with unobserved confounding. *arXiv preprint arXiv:2102.09412*.

Zheng, J., D'Amour, A., and Franks, A. (2022). Bayesian inference and partial identification in multi-treatment causal inference with unobserved confounding. In *International Conference on Artificial Intelligence and Statistics*, pages 3608–3626. PMLR.

Zheng, J., Wu, J., D'Amour, A., and Franks, A. (2023). Sensitivity to unobserved confounding in studies with factor-structured outcomes. *Journal of the American Statistical Association*, (just-accepted):1–23.

Zhou, Y., Tang, D., Kong, D., and Wang, L. (2020). The promises of parallel outcomes. *arXiv preprint arXiv:2012.05849*.

A Technical Details

A.1 Proofs of Proposition 1, and Theorems 1, 2, 3, and 4

Proof of Theorem 1. The omitted confounding bias is bounded as follows:

$$\begin{aligned}\text{Bias}_{a,t_1,t_2}^2 &= \left(a^\top \Gamma \Sigma_{u|t}^{-1/2} \mu_{u|\Delta t} \right)^2 \\ &= \|a^\top \Gamma\|_2^2 \|\Sigma_{u|t}^{-1/2} \mu_{u|\Delta t}\|_2^2 \cos^2(\theta_{a,t_1,t_2}) \\ &\leq \|a^\top \Gamma\|_2^2 \|\Sigma_{u|t}^{-1/2} \mu_{u|\Delta t}\|_2^2,\end{aligned}$$

where θ_{a,t_1,t_2} represents the angle between the vectors $a^\top \Gamma$ and $\Sigma_{u|t}^{-1/2} \mu_{u|\Delta t}$. This completes the proof, and the bound can be reached when $a^\top \Gamma$ is colinear with $\Sigma_{u|t}^{-1/2} \mu_{u|\Delta t}$. \square

Proof of Theorem 2. We first show the identification of $\|a^\top \Gamma\|_2$. Under the first condition of Assumption 4, $\Gamma \Gamma^\top$ and $\Sigma_{y|t,u}$ is uniquely determined from

$$\begin{aligned}\text{Cov}[Y - g(T)|T = t] &= \Gamma \Sigma_{u|t}^{-1/2} \text{Cov}(U|T = t) (\Gamma \Sigma_{u|t}^{-1/2})^\top + \text{Cov}(\epsilon_Y) \\ &= \Gamma \Sigma_{u|t}^{-1/2} \Sigma_{u|t} \Sigma_{u|t}^{-1/2} \Gamma^\top + \Sigma_{y|t,u} \\ &= \Gamma \Gamma^\top + \Sigma_{y|t,u},\end{aligned}$$

by applying Lemma 5.1 and Theorem 5.1 of Anderson and Rubin (1956), Γ is identified *up to rotations* from the right under the factor confounding assumption.

In other words, Γ is identified up to multiplication on the right by an orthogonal matrix, and thus any admissible value for Γ can be written as $\tilde{\Gamma} = \Gamma R$ with an arbitrary $m \times m$ orthogonal matrix R . Then $\|a^\top \tilde{\Gamma}\|_2$, which is rotation-invariant, is identified as follows.

$$\begin{aligned}\|a^\top \tilde{\Gamma}\|_2^2 &= \|a^\top \Gamma R\|_2^2 \\ &= a^\top \Gamma R (\Gamma R)^\top a \\ &= a^\top \Gamma \Gamma^\top a \\ &= \|a^\top \Gamma\|_2^2,\end{aligned}$$

since $RR^\top = I$.

Next, we show the identification of $\|\Sigma_{u|t}^{-1/2} \mu_{u|\Delta t}\|_2$, by applying the same idea to the treatment model. Under condition 2 of Assumption 4, BB^\top and $\Sigma_{t|u}$ are uniquely determined from $\text{Cov}(T) = BB^\top + \text{Cov}(\epsilon_t) = BB^\top + \Sigma_{t|u}$, and any admissible value for B can be written as $\tilde{B} = BR$ where R is again an arbitrary $m \times m$ orthogonal matrix. Then, the conditional distribution of U given T with \tilde{B} is

$$f_{\tilde{B}}(u|T = t) \sim N_m(\tilde{\mu}_{u|t}, \tilde{\Sigma}_{u|t}),$$

with

$$\begin{aligned}
\tilde{\mu}_{u|t} &= \tilde{B}^\top (\tilde{B}\tilde{B}^\top + \Sigma_{t|u})^{-1} t \\
&= R^\top B^\top (BB^\top + \Sigma_{t|u})^{-1} t \\
&= R^\top \mu_{u|t}, \\
\tilde{\Sigma}_{u|t} &= I_m - \tilde{B}^\top (\tilde{B}\tilde{B}^\top + \Sigma_{t|u})^{-1} \tilde{B} \\
&= I_m - R^\top B^\top (BB^\top + \Sigma_{t|u})^{-1} BR \\
&= R^\top \Sigma_{u|t} R.
\end{aligned}$$

Then, we can show that

$$\begin{aligned}
\|\tilde{\Sigma}_{u|t}^{-1/2} \tilde{\mu}_{u|\Delta t}\|_2^2 &= \|(R^\top \Sigma_{u|t} R)^{-1/2} (R^\top \mu_{u|\Delta t})\|_2^2 \\
&= \text{tr} \left\{ (R^\top \mu_{u|\Delta t})^\top (R^\top \Sigma_{u|t} R)^{-1} (R^\top \mu_{u|\Delta t}) \right\} \\
&= \text{tr} \left(\mu_{u|\Delta t}^\top \Sigma_{u|t}^{-1} \mu_{u|\Delta t} \right) \\
&= \|\Sigma_{u|t}^{-1/2} \mu_{u|\Delta t}\|_2^2,
\end{aligned}$$

where $RR^\top = I$, which implies that $\|\Sigma_{u|t}^{-1/2} \mu_{u|\Delta t}\|_2$ is identified. Combining the identification results, the bias bound is identifiable under the conditions of Assumption 4.

Lastly, we show that even though both B and Γ are only identifiable up to rotation, an equivalent representation of the bias allows us to treat \tilde{B} as the true value B and only focus on identifying the rotation matrix associated with Γ . Before doing this, let us first define the eigendecomposition $\Sigma_{u|t} = QAQ^{-1}$, which implies that $\Sigma_{u|t}^{-1/2} = QA^{-1/2}Q^{-1}$. We also define two separate rotation matrices for this calculation. We let R_1 be the rotation for Γ such that $\tilde{\Gamma} = \Gamma R_1$, and define R_2 so that $\tilde{B} = BR_2$. Using the relationships described above, it is easy to show that $\tilde{\Sigma}_{u|t}^{-1/2} = R_2^\top QA^{-1/2}Q^{-1}R_2 = R_2^\top \Sigma_{u|t}^{-1/2} R_2$. Putting this all together, we can write the bias as

$$\begin{aligned}
a^\top \Gamma \Sigma_{u|t}^{-1/2} \mu_{u|t} &= a^\top \tilde{\Gamma} R_1 \Sigma_{u|t}^{-1/2} \mu_{u|t} \\
&= a^\top \tilde{\Gamma} R_1 R_2 \tilde{\Sigma}_{u|t}^{-1/2} R_2^\top \mu_{u|t} \\
&= a^\top \tilde{\Gamma} R_1 R_2 \tilde{\Sigma}_{u|t}^{-1/2} R_2^\top R_2 \tilde{\mu}_{u|t} \\
&= a^\top \tilde{\Gamma} R_1 R_2 \tilde{\Sigma}_{u|t}^{-1/2} \tilde{\mu}_{u|t} \\
&= a^\top \tilde{\Gamma} R^* \tilde{\Sigma}_{u|t}^{-1/2} \tilde{\mu}_{u|t}
\end{aligned}$$

where $R^* = R_1 R_2$ is an orthogonal matrix, since the product of orthogonal matrices is also orthogonal. This shows that we can treat the \tilde{B} , $\tilde{\Sigma}_{u|t}^{-1/2}$, and $\tilde{\mu}_{u|t}$ parameters as the true values, and the only parameter off by rotation is $\tilde{\Gamma}$. □

Proof of Proposition 1 and Theorem 3. Here we focus on Theorem 3, but the result in Proposition 1 can be found as a special case of the result in Theorem 3 and therefore we do not provide an explicit proof. We assume that we only have a single negative control contrast. This provides us

information about the plausible values of $b_j^\top \Gamma$. To ensure that the negative control assumptions are compatible, the solution for (16) exists as

$$b_j^\top \Gamma = b_j^\top \check{\mathcal{G}}_j M_j^\dagger + w_{b,j}(I - M_j M_j^\dagger), \quad (20)$$

for some arbitrary m -dimensional row vector $w_{b,j}$, if and only if

$$b_j^\top \check{\mathcal{G}}_j M_j^\dagger M_j = b_j^\top \check{\mathcal{G}}_j$$

holds (Penrose, 1955), where M_j^\dagger denotes a generalized inverse of M_j , $M_j M_j^\dagger$ is the projection matrix onto the column space of M_j , and $M_j^\dagger M_j$ is the projection matrix onto the row space of M_j . Note here that if $c_j = m$, we have that M_j^\dagger is a standard inverse instead of a generalized inverse, and we are able to identify $b_j^\top \Gamma$.

We also have a different piece of information about the relationship between $a^\top \Gamma$ and $b_j^\top \Gamma$, which we have from our factor model assumptions. This is given by

$$b_j^\top \Gamma \Gamma^\top a = a^\top \Gamma \Gamma^\top b_j = k_{ab} \quad (21)$$

for some constant k_{ab} that is identified from our factor model assumptions. We can combine these two pieces of information to see that

$$a^\top \Gamma = k_{ab}(D^\top)^\dagger + w_a\{I - (D^\top)(D^\top)^\dagger\}, \quad (22)$$

where

$$D := b_j^\top \Gamma = b_j^\top \check{\mathcal{G}}_j M_j^\dagger + w_{b,j}(I - M_j M_j^\dagger)$$

is an m -dimensional row vector. Since D is a vector, we here use the fact that

$$D^\dagger = \frac{D^\top}{\|D\|_2^2} = \frac{D^\top}{\|b_j^\top \Gamma\|_2^2} = \frac{D^\top}{k_{bb}} \quad \text{and thus} \quad (D^\dagger)^\top = (D^\top)^\dagger = \frac{D}{k_{bb}},$$

where $k_{bb} := b_j^\top \Gamma \Gamma^\top b_j$ is an identifiable constant.

Combining these ideas together, for treatment contrast $\Delta t = t_1 - t_2$, we can see that the omitted variable bias of PATE_{a,t_1,t_2} is

$$\begin{aligned} \text{Bias}_{a,t_1,t_2} &= a^\top \Gamma \Sigma_{u|t}^{-1/2} \mu_{u|\Delta t} \\ &= k_{ab}(D^\top)^\dagger \Sigma_{u|t}^{-1/2} \mu_{u|\Delta t} + w_a\{I - (D^\top)(D^\top)^\dagger\} \Sigma_{u|t}^{-1/2} \mu_{u|\Delta t} \\ &= \frac{k_{ab}}{k_{bb}} b_j^\top \Gamma \Sigma_{u|t}^{-1/2} \mu_{u|\Delta t} + w_a\{I - (D^\top)(D^\top)^\dagger\} \Sigma_{u|t}^{-1/2} \mu_{u|\Delta t} \\ &= \underbrace{\frac{k_{ab}}{k_{bb}} b_j^\top \check{\mathcal{G}}_j M_j^\dagger \Sigma_{u|t}^{-1/2} \mu_{u|\Delta t}}_{\text{(I) bias correction}} + \underbrace{\frac{k_{ab}}{k_{bb}} w_{b,j}(I - M_j M_j^\dagger) \Sigma_{u|t}^{-1/2} \mu_{u|\Delta t}}_{\text{(II)}} \\ &\quad + \underbrace{w_a\{I - (D^\top)(D^\top)^\dagger\} \Sigma_{u|t}^{-1/2} \mu_{u|\Delta t}}_{\text{(III)}} \end{aligned}$$

The first term (I) is identifiable and is the *bias correction term* for the center of our new interval. Now all that is left to do is to bound (II) and (III), which include the free vectors w_a and $w_{b,j}$ and are therefore unidentifiable.

We can first bound (II). We can see that the l_2 norm of this vector is given by

$$\begin{aligned} & \left\| \frac{k_{ab}}{k_{bb}} w_{b,j} (I - M_j M_j^\dagger) \Sigma_{u|t}^{-1/2} \mu_{u|\Delta t} \right\|_2^2 \\ &= \left\| \frac{k_{ab}}{k_{bb}} w_{b,j} (I - M_j M_j^\dagger)^2 \Sigma_{u|t}^{-1/2} \mu_{u|\Delta t} \right\|_2^2 \\ &\leq \left\| \frac{k_{ab}}{k_{bb}} w_{b,j} (I - M_j M_j^\dagger) \right\|_2^2 \left\| (I - M_j M_j^\dagger) \Sigma_{u|t}^{-1/2} \mu_{u|\Delta t} \right\|_2^2, \end{aligned}$$

where the first equality holds because $(I - M_j M_j^\dagger)$ is an idempotent matrix. Taking the l_2 norm of both sides of (20) and re-arranging terms gives us that

$$\|w_{b,j} (I - M_j M_j^\dagger)\|_2^2 = \|b_j^\top \Gamma\|_2^2 - \|b_j^\top \check{\mathcal{G}}_j M_j^\dagger\|_2^2.$$

Hence,

$$\begin{aligned} |(II)| &\leq \left\| \frac{k_{ab}}{k_{bb}} w_{b,j} (I - M_j M_j^\dagger) \right\|_2 \left\| (I - M_j M_j^\dagger) \Sigma_{u|t}^{-1/2} \mu_{u|\Delta t} \right\|_2 \\ &= \left| \frac{k_{ab}}{k_{bb}} \right| \sqrt{k_{bb} - \|b_j^\top \check{\mathcal{G}}_j M_j^\dagger\|_2^2} \left\| (I - M_j M_j^\dagger) \Sigma_{u|t}^{-1/2} \mu_{u|\Delta t} \right\|_2, \end{aligned}$$

where we use the notation $k_{bb} = \|b_j^\top \Gamma\|_2^2$.

In a similar way, we can get an upper bound of (III). We here use the fact that

$$\begin{aligned} & \|w_a \{I - (D^\top)(D^\top)^\dagger\} \Sigma_{u|t}^{-1/2} \mu_{u|\Delta t}\|_2^2 \\ &= \|w_a \{I - (D^\top)(D^\top)^\dagger\}^2 \Sigma_{u|t}^{-1/2} \mu_{u|\Delta t}\|_2^2 \\ &\leq \|w_a \{I - (D^\top)(D^\top)^\dagger\}\|_2^2 \|\{I - (D^\top)(D^\top)^\dagger\} \Sigma_{u|t}^{-1/2} \mu_{u|\Delta t}\|_2^2 \end{aligned}$$

and, from (22),

$$\begin{aligned} \|w_a \{I - (D^\top)(D^\top)^\dagger\}\|_2^2 &= \|a^\top \Gamma\|_2^2 - \|k_{ab} (D^\top)^\dagger\|_2^2 \\ &= k_{aa} - \|k_{ab} (D^\top)^\dagger\|_2^2, \end{aligned}$$

where $k_{aa} := \|a^\top \Gamma\|_2^2$. To simplify this further, we use that

$$\|(D^\top)^\dagger\|_2^2 = \left\| \frac{D}{k_{bb}} \right\|_2^2 = \frac{1}{k_{bb}^2} \|D\|_2^2 = \frac{k_{bb}}{k_{bb}^2} = \frac{1}{k_{bb}}.$$

Combining all of this gives us our final bound on (III), which is given by

$$\begin{aligned} |(III)| &\leq \|w_a \{I - (D^\top)(D^\top)^\dagger\}\|_2 \|\{I - (D^\top)(D^\top)^\dagger\} \Sigma_{u|t}^{-1/2} \mu_{u|\Delta t}\|_2 \\ &\leq \sqrt{k_{aa} - \frac{k_{ab}^2}{k_{bb}^2}} \|\{I - (D^\top)(D^\top)^\dagger\} \Sigma_{u|t}^{-1/2} \mu_{u|\Delta t}\|_2 \\ &\leq \sqrt{k_{aa} - \frac{k_{ab}^2}{k_{bb}^2}} \|\Sigma_{u|t}^{-1/2} \mu_{u|\Delta t}\|_2. \end{aligned}$$

The final step is done because the $\|\{I - (D^\top)(D^\top)^\dagger\}\Sigma_{u|t}^{-1/2}\mu_{u|\Delta t}\|_2$ term is unidentifiable, which means that different rotations of either the Γ or B matrices can lead to different values of this quantity. Putting all of these thoughts together gives us the following interval for the confounding bias of $a^\top Y$ in the presence of the negative controls:

$$\begin{aligned} & \frac{k_{ab}}{k_{bb}} b_j^\top \check{\mathcal{G}}_j M_j^\dagger \Sigma_{u|t}^{-1/2} \mu_{u|\Delta t} \quad \pm \\ & \left(\left| \frac{k_{ab}}{k_{bb}} \right| \sqrt{k_{bb} - \|b_j^\top \check{\mathcal{G}}_j M_j^\dagger\|_2^2} \|(I - M_j M_j^\dagger) \Sigma_{u|t}^{-1/2} \mu_{u|\Delta t}\|_2 \right. \\ & \left. + \sqrt{k_{aa} - \frac{k_{ab}^2}{k_{bb}}} \|\Sigma_{u|t}^{-1/2} \mu_{u|\Delta t}\|_2 \right). \end{aligned}$$

Note that we obtain point identification of the treatment effect if (i) we have m negative control contrasts ($c_j = m$), and (ii) either our negative control outcome is the same as the outcome of interest ($a = b_j$) or $a^\top \Gamma$ is colinear with $b_j^\top \Gamma$. \square

Proof of Theorem 4. Here we prove the results of Section 5.3.2 and show that under the conditions of Theorem 4, we can write the bias as a known function of identifiable quantities. As a reminder, the two pieces of information we have in order to identify the bias are

$$a^\top \Gamma \Gamma^\top b = K_{ab} \tag{23}$$

$$b_j^\top \Gamma M_j = b_j^\top \check{\mathcal{G}}_j \text{ for } j = 1, \dots, J. \tag{24}$$

We prove the results separately by scenario, beginning with scenario 1:

Scenario 1: $a^\top \Gamma \in \mathcal{C}(\Gamma^\top b^*)$ and $b_j^\top \Gamma \in \mathcal{C}(M_j)$ for all $j \in \mathcal{J}^*$.

First, we need to verify that these two conditions are themselves verifiable despite only knowing Γ up to rotation. The first condition holds because $a^\top \Gamma \in \mathcal{C}(\Gamma^\top b^*)$ holds if and only if $a^\top \Gamma R \in \mathcal{C}(R^\top \Gamma^\top b^*)$ for orthogonal matrices R . The second condition holds because we know the inner product between $b_j^\top \Gamma$ and every column of M_j . This implies that we can check the inner product of $b_j^\top \Gamma$ and any linear combination of the columns in M_j and therefore we can check if $b_j^\top \Gamma$ lies in the span of M_j . The first condition implies that we can write

$$a^\top \Gamma = \sum_j w_j b_j^\top \Gamma$$

for some constants w_j for $j = 1, \dots, J^*$ that are identifiable since we know the inner product of $a^\top \Gamma$ with $b_j^\top \Gamma$ for all j . Letting M_{jk} be the k th column of M_j , the second condition implies that we can write

$$b_j^\top \Gamma = \sum_k d_{jk} M_{jk}^\top$$

for some constants d_{jk} for $k = 1, \dots, c_j$ that are identifiable because we know the inner product

between $b_j^\top \Gamma$ and each of M_{jk} . Putting this together, we can see that the bias is written as

$$\begin{aligned} a^\top \Gamma \Sigma_{u|t}^{-1/2} \mu_{u|\Delta t} &= \left(\sum_j w_j b_j^\top \Gamma \right) \Sigma_{u|t}^{-1/2} \mu_{u|\Delta t} \\ &= \sum_j \sum_k w_j d_{jk} M_{jk}^\top \Sigma_{u|t}^{-1/2} \mu_{u|\Delta t}, \end{aligned}$$

which is a fully identifiable quantity. This shows that the bias is a known function of identifiable quantities in this scenario.

Scenario 2: There exists a j such that $a^\top \Gamma$ is colinear with $b_j^\top \Gamma$ and $\Sigma_{u|t}^{-1/2} \mu_{u|\Delta t} \in \mathcal{C}(M_j)$.

Clearly we can check if $a^\top \Gamma$ is colinear with $b_j^\top \Gamma$ as this is invariant to rotation. Additionally, the second condition is straightforward to check as both $\Sigma_{u|t}^{-1/2} \mu_{u|\Delta t}$ and M_j are identifiable quantities and therefore we can check if $\Sigma_{u|t}^{-1/2} \mu_{u|\Delta t}$ lies in the span of the columns of M_j . Because of these two conditions, we can write

$$\begin{aligned} a^\top \Gamma &= w b_j^\top \Gamma \\ \Sigma_{u|t}^{-1/2} \mu_{u|\Delta t} &= \sum_k d_{jk} M_{jk} \end{aligned}$$

for identifiable constants w and d_{jk} for $k = 1, \dots, c_j$. This implies that the bias is identified as

$$a^\top \Gamma \Sigma_{u|t}^{-1/2} \mu_{u|\Delta t} = w \sum_k d_{jk} b_j^\top \Gamma M_{jk},$$

which is a fully identifiable quantity because we observe $b_j^\top \Gamma M_{jk}$ through the negative control assumption.

Scenario 3: $\Sigma_{u|t}^{-1/2} \mu_{u|\Delta t} \in \mathcal{C}(\Gamma^\top b^*)$ and $b_j^\top \Gamma \in \mathcal{C}(M_j)$ for all $j \in \mathcal{J}^*$.

Normally, it would not be possible to verify if $\Sigma_{u|t}^{-1/2} \mu_{u|\Delta t} \in \mathcal{C}(\Gamma^\top b^*)$ because Γ is only known up to rotation, which can affect its corresponding column space. However, the second condition is verifiable since we know the inner product between $b_j^\top \Gamma$ and each column of M_j from the negative control assumption, which allows us to check the inner product of $b_j^\top \Gamma$ with any linear combination of the columns of M_j . Given this second condition, we can write

$$b_j^\top \Gamma = \sum_k d_{jk} M_{jk}^\top,$$

for constants d_{jk} for $k = 1, \dots, c_j$ that are identifiable. Because we can write $b_j^\top \Gamma$ in terms of identifiable quantities for all $j \in \mathcal{J}^*$, we can check the first condition to see whether $\Sigma_{u|t}^{-1/2} \mu_{u|\Delta t} \in \mathcal{C}(\Gamma^\top b^*)$. If true, then we can write

$$\Sigma_{u|t}^{-1/2} \mu_{u|\Delta t} = \sum_j w_j b_j^\top \Gamma$$

for identifiable constants w_j for $j \in \mathcal{J}^*$. This leads to writing the bias as

$$\begin{aligned} a^\top \Gamma \Sigma_{u|t}^{-1/2} \mu_{u|\Delta t} &= a^\top \Gamma \sum_j w_j b_j^\top \Gamma \\ &= \sum_j w_j K_{ab_j}, \end{aligned}$$

which is identifiable from our factor confounding assumptions. \square

A.2 Extension to multiple negative controls

The previous results on negative controls only hold when there exists a single negative control pair, i.e., $J = 1$. We used this example as a starting point to provide intuition for the benefits that negative control pairs can provide, but having more negative control pairs can reduce the width of the partial identification region even further. We extend these results to settings with $J \geq 1$ in Theorem 5.

Theorem 5. *Under the assumptions of Theorem 3, suppose that we have J negative control outcomes where $1 \leq J \leq m$, and $c_j \leq m$ negative control contrasts for each outcome. We define $b = [b_1, b_2, \dots, b_J]$, to be a $q \times J$ matrix that has each individual b_j as its columns. Let $K_{ab} = a^\top \Gamma \Gamma^\top b$ be a J -dimensional row vector, and $K_{bb} = b^\top \Gamma \Gamma^\top b$ be a $J \times J$ matrix, both of which are identified from our factor model assumptions. Then the confounding bias, $Bias_{a,t_1,t_2}$, is in the interval*

$$\begin{aligned} K^* D^* \Sigma_{u|t}^{-1/2} \mu_{u|\Delta t} &\pm \\ \left(\sum_{j=1}^J |(K^*)_j| \sqrt{(K_{bb})_{j,j} - \|(D^*)_{j\cdot}\|_2^2} \|(I - M_j M_j^\dagger) \Sigma_{u|t}^{-1/2} \mu_{u|\Delta t}\|_2 \right. \\ &\left. + \sqrt{K_{aa} - \|K^* b^\top \Gamma\|_2^2} \|\Sigma_{u|t}^{-1/2} \mu_{u|\Delta t}\|_2 \right), \end{aligned} \quad (25)$$

where $(K^*)_j$ is the j th element of $K^* := K_{ab} K_{bb}^{-1}$, $(K_{bb})_{j,j}$ is the (j,j) th entry of K_{bb} , and $(D^*)_{j\cdot}$ is the j th row of a $J \times m$ matrix D^* , each row of which contains $b_j^\top \check{\mathcal{G}}_j M_j^\dagger$.

The intuition for the partial identification region in Theorem 5 is analogous to the case with a single negative control condition. Ideal negative control pairs are those with large confounding biases and whose treatment and outcome are affected by similar linear combinations of the unmeasured confounders as the treatment and outcome of interest, i.e., they have similar confounding mechanisms. We now give a proof of this result.

Proof of Theorem 5. Suppose that there are J outcomes with at least one negative control treatment. Letting $\mathcal{Q} \subset \{1, \dots, q\}$ denote a set of the indices of such outcomes and $\text{card}(\cdot)$ denote the cardinality of a set, we have that $J = \text{card}(\mathcal{Q})$. The negative control contrast provides us information about the plausible values of $b_j^\top \Gamma$ for $j \in \mathcal{Q}$. In particular, we can see the following. By Theorem 2 of Penrose (1955), a necessary and sufficient condition for (16) to have a solution is

$$b_j^\top \check{\mathcal{G}}_j M_j^\dagger M_j = b_j^\top \check{\mathcal{G}}_j,$$

in which case the general solution exists as

$$b_j^\top \Gamma = b_j^\top \check{\mathcal{G}}_j M_j^\dagger + w_{b,j} (I - M_j M_j^\dagger) \quad (26)$$

for some arbitrary m -dimensional row vector $w_{b,j}$, where M_j^\dagger denotes a generalized inverse of M_j , $M_j M_j^\dagger$ is the projection matrix onto the column space of M_j , and $M_j^\dagger M_j$ is the projection matrix onto the row space of M_j . Notice that (26) satisfies

$$\|w_{b,j} (I - M_j M_j^\dagger)\|_2^2 = \|b_j^\top \Gamma\|_2^2 - \|b_j^\top \check{\mathcal{G}}_j M_j^\dagger\|_2^2. \quad (27)$$

For notational convenience, we denote the decomposition of (26) by $b_j^\top \Gamma := D_j = D_j^{(1)} + D_j^{(2)}$ where $D_j^{(1)} := b_j^\top \check{\mathcal{G}}_j M_j^\dagger$ and $D_j^{(2)} := w_{b,j}(I - M_j M_j^\dagger)$. It will also be useful later to break this matrix into two components since $D^{(1)}$ contains the estimable components and $D^{(2)}$ refers to the unidentified portion. We refer to the stacked version of D_j 's as $\mathbf{D} = [D_1^\top, \dots, D_J^\top]^\top$, which is a $J \times m$ matrix. We can also define $\mathbf{b} = [b_1, b_2, \dots, b_J]$, which is a $q \times J$ matrix that has each individual b_j as its columns. In other words, in the matrix form, we have that

$$\begin{pmatrix} b_1^\top \Gamma \\ \vdots \\ b_J^\top \Gamma \end{pmatrix} = \begin{pmatrix} b_1^\top \check{\mathcal{G}}_1 M_1^\dagger + w_{b,1}(I - M_1 M_1^\dagger) \\ \vdots \\ b_J^\top \check{\mathcal{G}}_J M_J^\dagger + w_{b,J}(I - M_J M_J^\dagger) \end{pmatrix} = \begin{pmatrix} D_1^{(1)} + D_1^{(2)} \\ \vdots \\ D_J^{(1)} + D_J^{(2)} \end{pmatrix} = \begin{pmatrix} D_1 \\ \vdots \\ D_J \end{pmatrix},$$

i.e., $\mathbf{b}^\top \Gamma = \mathbf{D}^{(1)} + \mathbf{D}^{(2)} = \mathbf{D}$.

Under our factor modeling assumptions, we are able to identify

$$a^\top \Gamma \Gamma^\top \mathbf{b} := K_{ab} \quad (28)$$

where K_{ab} is a J -dimensional row vector. Using the fact that $\mathbf{b}^\top \Gamma = \mathbf{D}$, we know that $a^\top \Gamma \mathbf{D}^\top := K_{ab}$, and thus all solutions to $a^\top \Gamma$ can be written as

$$a^\top \Gamma = K_{ab}(\mathbf{D}^\top)^\dagger + w_a \left\{ I - (\mathbf{D}^\top)(\mathbf{D}^\top)^\dagger \right\} \quad (29)$$

for some arbitrary m -dimensional row vector w_a . This follows

$$\left\| w_a \left\{ I - (\mathbf{D}^\top)(\mathbf{D}^\top)^\dagger \right\} \right\|_2^2 = \|a^\top \Gamma\|_2^2 - \|K_{ab}(\mathbf{D}^\top)^\dagger\|_2^2. \quad (30)$$

Given that the rank of \mathbf{D} is J , we can re-write \mathbf{D}^\dagger as

$$\mathbf{D}^\dagger = \mathbf{D}^\top (\mathbf{D} \mathbf{D}^\top)^{-1}$$

and $(\mathbf{D}^\top)^\dagger = (\mathbf{D}^\dagger)^\top = (\mathbf{D} \mathbf{D}^\top)^{-1} \mathbf{D}$, which implies that

$$\begin{aligned} a^\top \Gamma &= K_{ab}(\mathbf{D} \mathbf{D}^\top)^{-1} \mathbf{D} + w_a \left\{ I - (\mathbf{D}^\top)(\mathbf{D}^\top)^\dagger \right\} \\ &= K_{ab}(\mathbf{D} \mathbf{D}^\top)^{-1} \mathbf{D}^{(1)} + K_{ab}(\mathbf{D} \mathbf{D}^\top)^{-1} \mathbf{D}^{(2)} + w_a \left\{ I - (\mathbf{D}^\top)(\mathbf{D}^\top)^\dagger \right\}. \end{aligned}$$

The bias for the estimand of interest is given by

$$\begin{aligned} &a^\top \Gamma \Sigma_{u|t}^{-1/2} \mu_{u|\Delta t} \\ &= K_{ab}(\mathbf{D} \mathbf{D}^\top)^{-1} \mathbf{D}^{(1)} \Sigma_{u|t}^{-1/2} \mu_{u|\Delta t} + K_{ab}(\mathbf{D} \mathbf{D}^\top)^{-1} \mathbf{D}^{(2)} \Sigma_{u|t}^{-1/2} \mu_{u|\Delta t} + w_a \left\{ I - (\mathbf{D}^\top)(\mathbf{D}^\top)^\dagger \right\} \Sigma_{u|t}^{-1/2} \mu_{u|\Delta t} \\ &= \underbrace{K_{ab} K_{bb}^{-1} \mathbf{D}^{(1)} \Sigma_{u|t}^{-1/2} \mu_{u|\Delta t}}_{(I) \text{ bias correction}} + \underbrace{K_{ab}(\mathbf{D} \mathbf{D}^\top)^{-1} \mathbf{D}^{(2)} \Sigma_{u|t}^{-1/2} \mu_{u|\Delta t}}_{(II)} + \underbrace{w_a \left\{ I - (\mathbf{D}^\top)(\mathbf{D}^\top)^\dagger \right\} \Sigma_{u|t}^{-1/2} \mu_{u|\Delta t}}_{(III)}, \end{aligned}$$

where $K_{bb} := \mathbf{D} \mathbf{D}^\top$, and thus the first term (I) is identifiable as our bias correction. The remaining two terms, (II) and (III), are not identifiable and therefore we will bound them to create regions for

the confounding bias that are compatible with the negative control conditions. Before bounding these terms, it is helpful to write (II) as

$$(II) = \sum_{j=1}^J \alpha_j w_{b,j} (I - M_j M_j^\dagger) \Sigma_{u|t}^{-1/2} \mu_{u|\Delta t},$$

where α_j is the j th element of the J -dimensional row vector $K_{ab}(\mathbf{D}\mathbf{D}^\top)^{-1} = K_{ab}K_{bb}^{-1}$. We know that, for $j = 1, \dots, J$,

$$\begin{aligned} & \left\{ \alpha_j w_{b,j} (I - M_j M_j^\dagger) \Sigma_{u|t}^{-1/2} \mu_{u|\Delta t} \right\}^2 \\ &= \left\{ \alpha_j w_{b,j} (I - M_j M_j^\dagger)^2 \Sigma_{u|t}^{-1/2} \mu_{u|\Delta t} \right\}^2 \\ &= \|\alpha_j w_{b,j} (I - M_j M_j^\dagger)^2 \Sigma_{u|t}^{-1/2} \mu_{u|\Delta t}\|_2^2 \\ &\leq \alpha_j^2 \|w_{b,j} (I - M_j M_j^\dagger)\|_2^2 \|(I - M_j M_j^\dagger) \Sigma_{u|t}^{-1/2} \mu_{u|\Delta t}\|_2^2. \end{aligned}$$

The first equality holds because $(I - M_j M_j^\dagger)$ is an idempotent matrix. Combining this with (27),

$$\begin{aligned} |(II)| &\leq \sum_{j=1}^J |\alpha_j| \|w_{b,j} (I - M_j M_j^\dagger)\|_2 \|(I - M_j M_j^\dagger) \Sigma_{u|t}^{-1/2} \mu_{u|\Delta t}\|_2 \\ &= \sum_{j=1}^J |\alpha_j| \sqrt{\|b_j^\top \Gamma\|_2^2 - \|b_j^\top \check{\mathcal{G}}_j M_j^\dagger\|_2^2} \|(I - M_j M_j^\dagger) \Sigma_{u|t}^{-1/2} \mu_{u|\Delta t}\|_2, \end{aligned}$$

where $\|b_j^\top \Gamma\|_2^2 = (K_{bb})_{j,j}$ is the (j, j) th entry of K_{bb} , which is identifiable.

Now we need to provide a bound for the final term (III) in the expression for the bias of interest. In a similar way, this can be done with (30) as,

$$\begin{aligned} |(III)| &\leq \left\| w_a \left\{ I - (\mathbf{D}^\top)(\mathbf{D}^\top)^\dagger \right\} \right\|_2 \left\| \left\{ I - (\mathbf{D}^\top)(\mathbf{D}^\top)^\dagger \right\} \Sigma_{u|t}^{-1/2} \mu_{u|\Delta t} \right\|_2 \\ &= \sqrt{K_{aa} - \|K_{ab}K_{bb}^{-1} \mathbf{b}^\top \Gamma\|_2^2} \left\| \left\{ I - (\mathbf{D}^\top)(\mathbf{D}^\top)^\dagger \right\} \Sigma_{u|t}^{-1/2} \mu_{u|\Delta t} \right\|_2 \\ &\leq \sqrt{K_{aa} - \|K_{ab}K_{bb}^{-1} \mathbf{b}^\top \Gamma\|_2^2} \|\Sigma_{u|t}^{-1/2} \mu_{u|\Delta t}\|_2, \end{aligned}$$

where $K_{aa} := a^\top \Gamma \Gamma^\top a$ is identifiable and $K_{ab}(\mathbf{D}^\top)^\dagger = K_{ab}K_{bb}^{-1} \mathbf{b}^\top \Gamma$. Putting all of this together, we can see that the confounding bias is in the region given by

$$\begin{aligned} & K_{ab}K_{bb}^{-1} \mathbf{D}^{(1)} \Sigma_{u|t}^{-1/2} \mu_{u|\Delta t} \quad \pm \\ & \left(\sum_{j=1}^J |\alpha_j| \sqrt{\|b_j^\top \Gamma\|_2^2 - \|b_j^\top \check{\mathcal{G}}_j M_j^\dagger\|_2^2} \|(I - M_j M_j^\dagger) \Sigma_{u|t}^{-1/2} \mu_{u|\Delta t}\|_2 \right. \\ & \quad \left. + \sqrt{K_{aa} - \|K_{ab}K_{bb}^{-1} \mathbf{b}^\top \Gamma\|_2^2} \|\Sigma_{u|t}^{-1/2} \mu_{u|\Delta t}\|_2 \right), \end{aligned}$$

which is equivalent to

$$\begin{aligned}
& K^* \mathbf{D}^* \Sigma_{u|t}^{-1/2} \mu_{u|\Delta t} \quad \pm \\
& \left(\sum_{j=1}^J |(K^*)_j| \sqrt{(K_{bb})_{j,j} - \|(\mathbf{D}^*)_{j\cdot}\|_2^2} \|(I - M_j M_j^\dagger) \Sigma_{u|t}^{-1/2} \mu_{u|\Delta t}\|_2 \right. \\
& \left. + \sqrt{K_{aa} - \|K^* \mathbf{b}^\top \Gamma\|_2^2} \|\Sigma_{u|t}^{-1/2} \mu_{u|\Delta t}\|_2 \right),
\end{aligned}$$

where $K^* := K_{ab} K_{bb}^{-1}$ and $\mathbf{D}^* := \mathbf{D}^{(1)}$. \square

B Algorithm for numerical approach in Section 5.3.1

We here outline the algorithm used to numerically determine the negative control partial identification regions. Note that we aim to minimize

$$\mathcal{F}(\tilde{R}) = (a^\top \tilde{\Gamma} \tilde{R} \Sigma_{u|t}^{-1/2} \mu_{u|\Delta t} - \beta)^2 + \sum_{j=1}^J \|b_j^\top \tilde{\Gamma} \tilde{R} M_j - b_j^\top \check{\mathcal{G}}_j\|_2^2,$$

with

$$\begin{aligned}
\nabla_{\tilde{R}} \mathcal{F}(\tilde{R}) = & 2 \left\{ \tilde{\Gamma}^\top a a^\top \tilde{\Gamma} \tilde{R} (\Sigma_{u|t}^{-1/2} \mu_{u|\Delta t}) (\Sigma_{u|t}^{-1/2} \mu_{u|\Delta t})^\top - \beta \tilde{\Gamma}^\top a (\Sigma_{u|t}^{-1/2} \mu_{u|\Delta t}) \right\} + \\
& 2 \sum_{j=1}^J (\tilde{\Gamma}^\top b_j b_j^\top \tilde{\Gamma} \tilde{R} M_j M_j^\top - \tilde{\Gamma}^\top b_j b_j^\top \check{\mathcal{G}}_j M_j^\top),
\end{aligned}$$

where $\tilde{R} \in \mathcal{V}_{m,m}$, the Stiefel manifold of all $m \times m$ orthogonal matrices. In order to run the algorithm, we first need to (i) specify t_1, t_2 , and a for the estimand of interest, and $\mathbf{b} = (b_1, \dots, b_J)$ for the negative control contrasts, (ii) obtain $\tilde{\Gamma}, \hat{\Sigma}_{u|t}, \hat{\mu}_{u|\Delta t}, \check{g}(\cdot), M_j$, and $b_j^\top \check{\mathcal{G}}_j$ for $j = 1, \dots, J$ using the estimation method described in Appendix C, (iii) define $\Theta = \{\theta_{a,t_1,t_2} : -1 \leq \cos(\theta_{a,t_1,t_2}) \leq 1\}$, a set of all candidate values of θ_{a,t_1,t_2} , and (iv) specify a threshold value, δ , as a selection criterion for θ_{a,t_1,t_2} . Note that under the notation introduced in Section 5.3.1, $\delta = \delta_1 = \delta_2/J$. Then the algorithm can be summarized in Algorithm 1. The idea is to find θ_{a,t_1,t_2} values that align with the conditions mentioned in Section 5.3.1. Once Algorithm 1 is implemented, we obtain Θ_{NC} and then construct the negative control partial identification region for bias as follows:

$$\text{Bias}_{a,t_1,t_2} \in \left\{ \|a^\top \Gamma\|_2 \|\Sigma_{u|t}^{-1/2} \mu_{u|\Delta t}\|_2 \cos(\theta_{a,t_1,t_2}) : \theta_{a,t_1,t_2} \in \Theta_{NC} \right\}.$$

Algorithm 1: Algorithm for finding negative control partial identification region

Input: t_1, t_2, a (estimand of interest), $\widehat{\Gamma}, \widehat{\Sigma}_{u|t}, \widehat{\mu}_{u|\Delta t}$ (estimates), $\mathbf{b}, M_j, b_j^\top \check{\mathcal{G}}_j, j = 1, \dots, J$ (negative controls), Θ (a set of candidate values of θ_{a,t_1,t_2}), δ (threshold value).

Output: Θ_{NC} , a set of all selected values of θ_{a,t_1,t_2} .

Initialize \tilde{R}_0 , by generating a random orthogonal matrix from the uniform distribution on the Stiefel manifold using the `rustiefel` function of the `rstiefel` package.

Initialize $\Theta_{NC} \leftarrow \emptyset$ (an empty set).

for each $\theta_{a,t_1,t_2} \in \Theta$ **do**

 Compute $\beta \leftarrow \|a^\top \widehat{\Gamma}\|_2 \|\widehat{\Sigma}_{u|t}^{-1/2} \widehat{\mu}_{u|\Delta t}\|_2 \cos(\theta_{a,t_1,t_2})$.

 Update $\tilde{R}^* \leftarrow \arg \min_{\tilde{R} \in \mathcal{V}_{m,m}} \mathcal{F}(\tilde{R})$ using the `optStiefel` function of the `rstiefel` package, with \tilde{R}_0 as the initial value and all unknown parameters replaced with their estimates.

if $(a^\top \widehat{\Gamma} \tilde{R}^* \widehat{\Sigma}_{u|t}^{-1/2} \widehat{\mu}_{u|\Delta t} - \beta)^2 \leq \delta$ **and** $\frac{1}{J} \sum_{j=1}^J \|b_j^\top \widehat{\Gamma} \tilde{R}^* M_j - b_j^\top \check{\mathcal{G}}_j\|_2^2 \leq \delta$ **then**

 | Add θ_{a,t_1,t_2} to the set Θ_{NC} .

end

 Set $\tilde{R}_0 \leftarrow \tilde{R}^*$.

end

C Estimation and inference on bounds

In this section, we describe our estimation procedure for the required statistical models, as well as an inferential procedure that accounts for sampling uncertainty when working with partial identification regions or bounds. For now, we assume $\Sigma_u = I_m$, $\Sigma_{t|u} = \sigma_{t|u}^2 I_k$, and $\Sigma_{y|t,u} = \sigma_{y|t,u}^2 I_q$, though it is relatively straightforward to adapt these strategies to non-equal variances.

C.1 Estimation of factor model parameters

The parameters corresponding to the treatment model, $\mu_{u|t}$ and $\Sigma_{u|t}$, can be estimated using factor analysis on the observed treatment matrix. From the treatment model, we have that

$$\text{Cov}(T) = BB^\top + \Sigma_{t|u},$$

where we want to estimate B and $\Sigma_{t|u}$. With a pre-specified number of factors, factor analysis can be applied to the covariance matrix of a standardized version of T , or the correlation matrix of T , which gives B^* and $\Sigma_{t|u}^*$, from

$$\text{Cor}(T) = B^* B^{*\top} + \Sigma_{t|u}^*.$$

Here, B^* is a matrix consisting of the factor loadings and $\Sigma_{t|u}^* = \text{diag}(\lambda_{t,1}^*, \dots, \lambda_{t,k}^*)$ is a diagonal matrix whose entries are the uniquenesses of each standardized treatment, which can be obtained from standard statistical software such as the `factanal` function in R. Letting $\sigma_{t,j}^2$ indicate the variance of the j th treatment, and setting $W = \text{diag}(\sigma_{t,1}^2, \dots, \sigma_{t,k}^2)$, we have that

$$\begin{aligned} \text{Cov}(T) &= W^{1/2} \text{Cor}(T) W^{1/2} \\ &= W^{1/2} B^* B^{*\top} W^{1/2} + W^{1/2} \Sigma_{t|u}^* W^{1/2} \\ &= (W^{1/2} B^*) (W^{1/2} B^*)^\top + W^{1/2} \Sigma_{t|u}^* W^{1/2}. \end{aligned}$$

Hence, we can obtain estimates of B and $\Sigma_{t|u}$ as follows:

$$\widehat{B} = \widehat{W}^{1/2} \widehat{B}^*,$$

$$\widehat{\Sigma}_{t|u} = \widehat{\sigma}_{t|u}^2 I_k = \frac{1}{k} \sum_{j=1}^k \widehat{\lambda}_{t,j}^* \widehat{\sigma}_{t,j}^2 I_k.$$

Note that it is straightforward to extend the estimate of $\Sigma_{t|u}$ to allow for unequal variances by using $\widehat{\Sigma}_{t|u} = W^{1/2} \Sigma_{t|u}^* W^{1/2}$, which we do in the analysis of PM_{2.5} components. This provides the parameter estimates of the latent confounder model for a given t :

$$\widehat{\mu}_{u|t} = \widehat{B}^\top (\widehat{B} \widehat{B}^\top + \widehat{\Sigma}_{t|u})^{-1} t,$$

$$\widehat{\Sigma}_{u|t} = I_m - \widehat{B}^\top (\widehat{B} \widehat{B}^\top + \widehat{\Sigma}_{t|u})^{-1} \widehat{B}.$$

The outcome model follows in a very similar way, though it requires an additional step where we first remove the effect of the treatment on the outcome. Specifically, we first estimate $\check{g}(\cdot)$ using a regression of Y on T , and compute $Y - \check{g}(T)$. We then perform the same factor analysis steps as for the treatment model, but on the correlation matrix of $Y - \check{g}(T)$, which will provide an estimate $\widehat{\Gamma}$ of the unknown factor loadings. Once we have obtained estimates \widehat{B} and $\widehat{\Gamma}$, we immediately obtain estimates of any identified quantity such as the partial R^2 values between the unmeasured confounders and treatment or outcome, as well as the bias bounds seen in Theorem 1.

One key component of factor analysis is determining how many factors to retain, as it is generally unknown in real applications. This is a well studied problem in the factor analysis literature, and there are a number of existing methods for determining the number of factors. Possibilities include the very simple structure criterion with complexity 1 and 2 (Revelle and Rocklin, 1979), the minimum average partial criterion (Velicer, 1976), BIC, adjusted BIC, including the number of factors with eigenvalues greater than those of random data (parallel analysis), or the number of eigenvalues greater than 1. We leave discussion to the merits of each of these approaches to the existing literature on factor analysis, though empirically we have found both BIC and factor analysis to work reasonably well in the simulations explored in our work. We recommend favoring too many factors instead of too few factors as this will generally lead to more conservative inferences. In the analysis of PM_{2.5} components, we used the largest number of factors allowable with 6 exposures and 6 outcomes, which is $m = 3$.

C.2 Statistical inference on bounds

Throughout the manuscript we have focused on population level quantities while ignoring the presence of sampling variability stemming from the estimation of unknown parameters. Standard inferential procedures used for point estimation do not immediately apply in this setting where we instead are targeting bounds for treatment effects. In this section, we describe a procedure based on the standard bootstrap in order to obtain upper and lower intervals for estimands of interest that have similar operating characteristics as standard confidence intervals in that they contain the true parameter $(1 - \alpha)100\%$ of the time across repeated samples of the data. Suppose that we estimate all parameters of interest across H bootstrap samples, where H is large. This provides us with bootstrap samples of all unknown parameters denoted by $\widehat{g}^{(h)}(\cdot)$, $\widehat{\Gamma}^{(h)}$, and $\widehat{B}^{(h)}$ for $h = 1, \dots, H$. From these values of the model parameters, we can use the aforementioned procedures to obtain bounds for our estimand of interest, which we denote by $(\widehat{I}_l^{(h)}, \widehat{I}_u^{(h)})$ for $h = 1, \dots, H$. Given these

bounds for each bootstrap sample, we can obtain the final bound $(\widehat{I}_l, \widehat{I}_u)$ to be the smallest bound such that $(1 - \alpha)100\%$ of the individual bootstrap bounds, $(\widetilde{I}_l^{(h)}, \widetilde{I}_u^{(h)})$ are fully contained within the interval.

Note that an analogous procedure could be done if the model parameters were all estimated within the Bayesian paradigm. For each posterior sample of the model parameters, we could calculate bounds, and then our final posterior bounds would be the smallest bounds that contain the desired proportion of the individual posterior sample bounds.

D Details of simulation study

Here we provide more explicit details on the data generation mechanism used in the simulation study of Section 6. As mentioned in the manuscript, we use a single data set of size $n = 10^6$ to effectively eliminate sampling variability and focus on uncertainty due to unmeasured confounding, and examine how partial identification regions change under varying assumptions. We set $m = 3$, $q = 6$, and $k = 10$. The relevant covariance matrices have values $\Sigma_u = I_m$, $\Sigma_{t|u} = 2I_k$, and $\Sigma_{yt|t,u} = 270I_q$. The true values of the coefficients relating the unmeasured variables U to both treatments and outcomes can be found in Figure 6, where we standardize each row by dividing by the residual standard deviation for that treatment or outcome to ensure each row is on the same scale. We generate the outcome to be a linear function of the treatments, and the values of these coefficients can be found in Figure 7. We also utilize a linear model for estimating the coefficients of the $\check{g}(\cdot)$ function, though the coefficients will be biased due to the presence of unmeasured confounding. The estimand of interest throughout is the effect of a one unit change for the 2nd treatment on the 2nd outcome. The first negative control outcome we use is the effect of the 2nd exposure on the first outcome, the negative control pair we use is the effect of the 3rd exposure on the 3rd outcome, and the double negative control outcome case uses the effect of the 2nd exposure on both the 1st and 6th outcomes as negative controls.

A number of useful insights about the simulation design can be seen from these figures. For one, we can see why the negative control pair (3rd exposure on the 3rd outcome) is a better negative control than the first negative control outcome (2nd exposure on the 1st outcome) when aiming to estimate the effect of the 2nd exposure on the 2nd outcome. The 1st and 2nd rows of the Γ matrix are nearly orthogonal, leading to a negative control that provides less information on the estimand of interest, while the 2nd and 3rd rows of Γ have a large, negative inner product, leading to a larger reduction in the size of the partial identification region. The values of B and Γ also provide insight into the degree of unmeasured confounding bias. The partial R-squared values between each treatment and the unmeasured confounders range from 0.7 to 0.8, while the analogous partial R-squared values for the outcome range from 0.15 to 0.73. This shows that the simulation captures a situation with a large degree of potential confounding bias, which highlights the utility of the different assumptions (negative controls, effect size constraints, and partial R-squared constraints) that are able to reduce the size of the partial identification region considerably despite the magnitude of the B and Γ coefficients.

E Additional results in Medicare analysis

Here we present additional results on the effects of air pollutants on public health outcomes in the Medicare cohort. First, we show results for elemental carbon, ammonium, ozone, and sulfates,

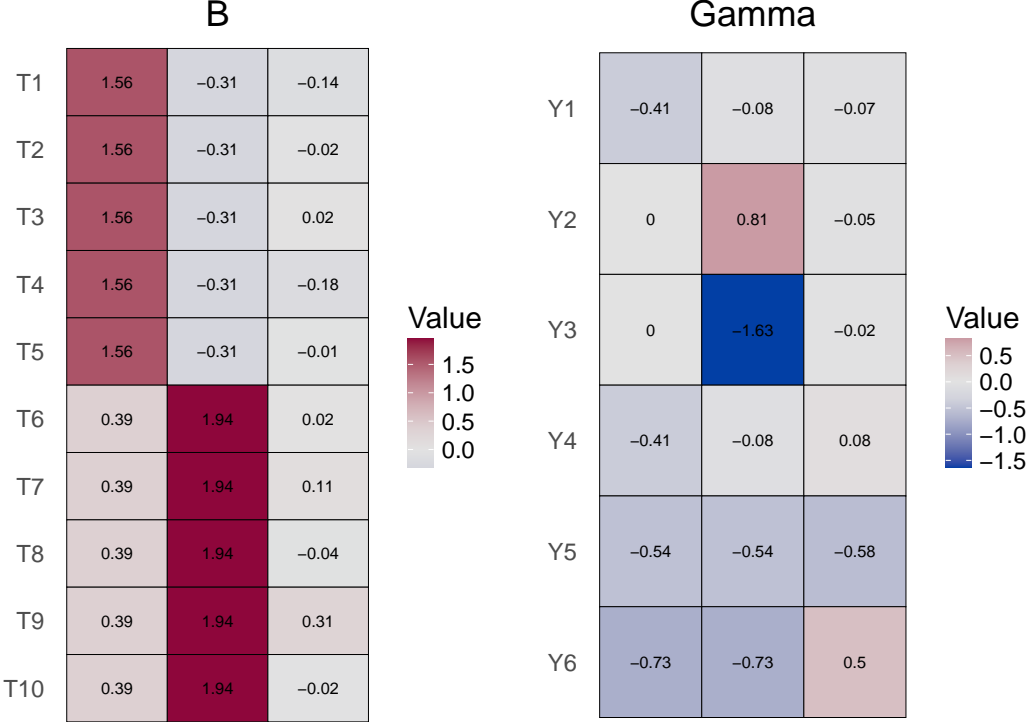


Figure 6: True values for the B and Γ matrices in the simulation study.

which were excluded from the main manuscript. We then show results with a less restrictive, symmetric effect size constraint for the effects of organic carbon.

E.1 Effects on other exposures

In this section, we show results under the same constraints as in the manuscript, but for the remaining exposures that consist of elemental carbon, ammonium, ozone, and sulfates. The results can be found in Figure 8. We see very wide partial identification regions for elemental carbon and ammonium, which is expected given the exceedingly large values of $R_{d^\top T \sim U|X}^2$ for these two exposures, which were 0.985 and 0.99, respectively. Similar results were found for sulfates, though the partial identification regions for this exposure are smaller in width. These findings show that it is unlikely within this framework to see informative partial identification regions under the shared confounding assumption when there is very strong dependence across exposures or outcomes. Nearly all of the unexplained variation in elemental carbon and ammonium are attributed to confounding in this situation, making it difficult to rule out large values of confounding bias. As a reminder, the confounding bias for the minimal sufficient confounder in Section 5.2 is given by

$$\text{Bias}_{a,t_1,t_2}^2 = R_{a^\top Y \sim U_{a,d}|T}^2 \frac{R_{d^\top T \sim U_{a,d}}^2}{1 - R_{d^\top T \sim U_{a,d}}^2} \frac{a^\top \Sigma_{y|t} a}{d^\top \Sigma_t d}.$$

Given that $1 - R_{d^\top T \sim U_{a,d}}^2$ is in the denominator of this expression, it is clear that large amounts of confounding bias are difficult to rule out with such large partial R-squared values for the exposures. Ozone presents the opposite situation, as it has a very small value of $R_{d^\top T \sim U|X}^2$, and subsequently has very small partial identification regions. This points to the fact that the shared confounding

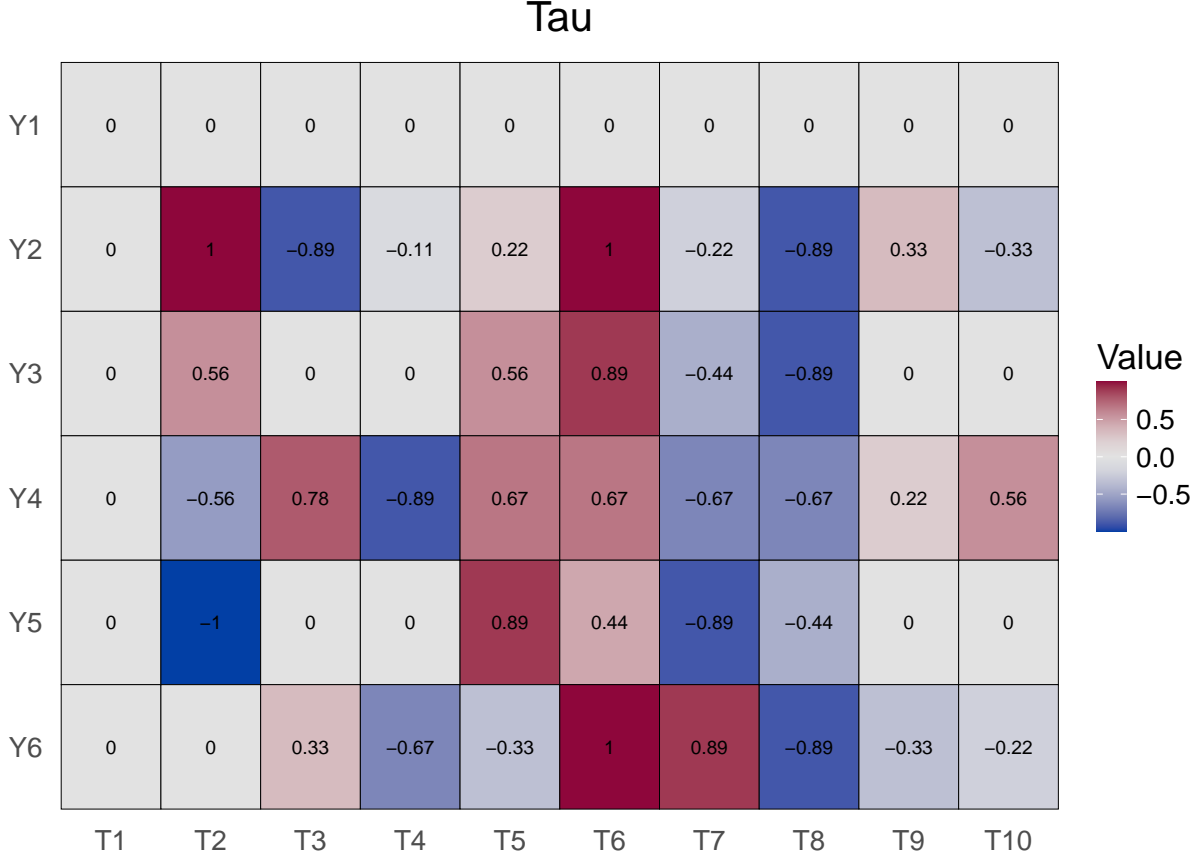


Figure 7: True values for the effect of each exposure on each outcome in the simulation study.

assumption may be less plausible for ozone compared with the other exposures that have stronger dependence.

E.2 Other effect size constraints

We now explore whether results are sensitive to the choice of effect size constraints. For this section, we focus on the results for organic carbon as this was the exposure for which we identified a harmful effect of pollution, even after accounting for the potential presence of unmeasured confounding. The partial identification regions for the other exposures were fairly wide and contained zero, and this remains true even when we change the upper and lower bounds of the effect size constraint. In the manuscript, we set $z_l = -0.05$ and $z_u = 0.2$, but we now explore a symmetric constraint where we set $z_l = -0.2$ and $z_u = 0.2$. The results for the causal effect of organic carbon under this constraint can be found in Figure 9. We see that results are insensitive to this choice and the significant effects of organic carbon on both COPD and stroke remain regardless of the constraint. We see that the more relaxed, symmetric constraint provides no additional information beyond what is provided by the negative control on prior COPD, leading to identical intervals for the two sets of constraints considered.

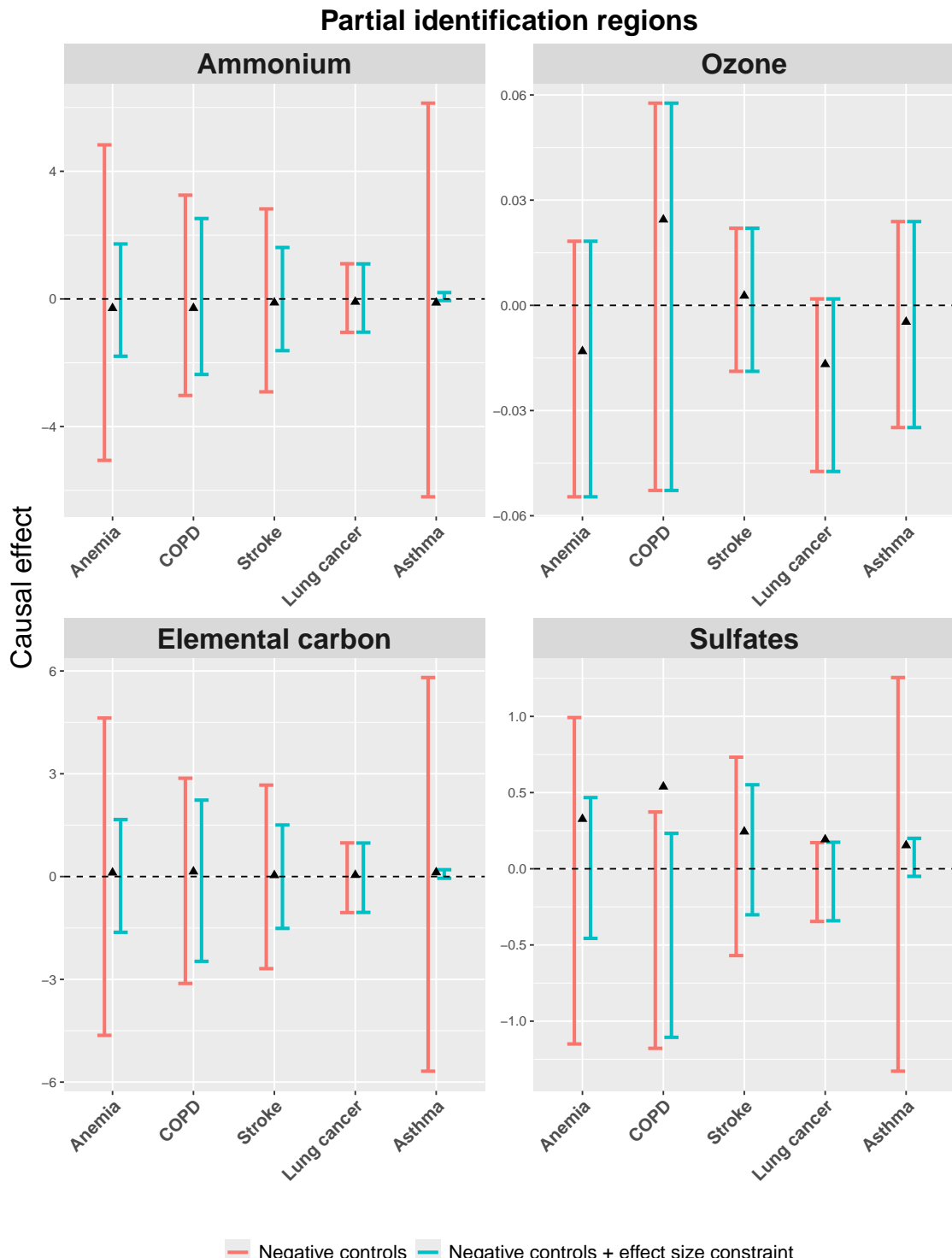


Figure 8: Partial identification regions for the causal effect of different exposures under the negative control and effect size constraints used in the manuscript. The triangles represent the estimates obtained assuming no unmeasured confounding.

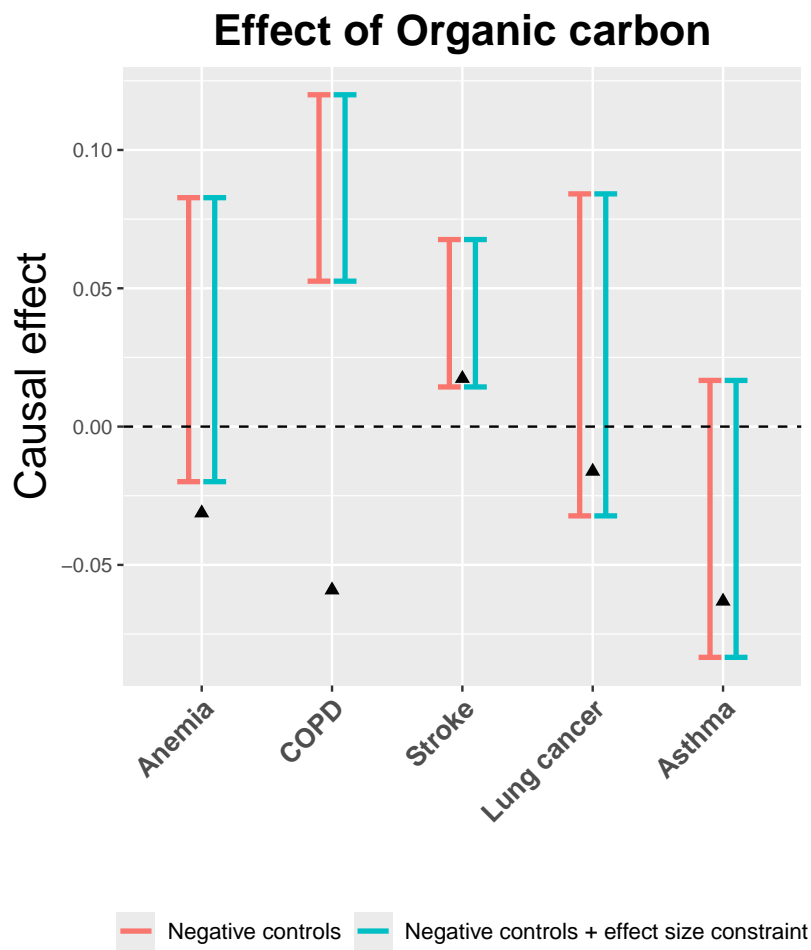


Figure 9: Partial identification regions for the causal effect of organic carbon under a symmetric effect size constraint with $z_l = -0.2$ and $z_u = 0.2$. The triangles represent the estimates obtained assuming no unmeasured confounding.